International Journal of Robust and Nonlinear Control

WILEY

RESEARCH ARTICLE OPEN ACCESS

Remaining Useful Life (RUL) Control of Controlled Systems Under Degradation

Mônica S. Félix | John J. Martinez | Christophe Bérenguer

University Grenoble Alpes, CNRS, Grenoble-INP, GIPSA-Lab, Institute of Engineering University of Grenoble Alpes, Grenoble, France

Correspondence: John J. Martinez (john.martinez@gipsa-lab.fr)

Received: 4 June 2024 | **Revised:** 9 June 2025 | **Accepted:** 11 July 2025

Funding: The authors received no specific funding for this work.

Keywords: health-aware control | prognostic and health management | Remaining Useful Life | wind turbine

ABSTRACT

Remaining Useful Life (RUL) is the length of time a component or system will operate before it requires repair or replacement. Although significant efforts have been made to estimate RUL accurately, controlling RUL remains challenging. This study introduces a state-space model-based approach for designing RUL controllers of controlled systems in degradation. It explores the relationship between a system's operational dynamics and its ongoing aging process, particularly the degradation rate experienced by a component during a given operational condition. In this approach, the RUL control problem is formulated as the problem of controlling a polytopic uncertain system. Therefore, robust design methods are proposed for both state observation and control to manage the degradation trajectory, ensuring an acceptable level of deterioration within a desired average lifetime. To illustrate its applicability, the proposed approach is implemented in a variable-speed wind turbine, with a flexible shaft subject to torsional effects. The results highlight the benefits of using RUL control to enhance the durability of controlled systems while maintaining production performance and demonstrate the effectiveness of such an approach for managing the system's end-of-life.

1 | Introduction

In reliability theory, it is well-established that systems degrade over time, leading to reduced performance and eventual failure [1]. This degradation affects critical factors such as safety, maintenance costs, and operation time. For example, in the wind turbine energy sector, maintenance costs can comprise a significant portion, approximately 20%, of total expenses [2]. Implementing strategies to manage system health is thus essential for reducing costs and ensuring sustained operation [3]. Health-aware Control (HAC) strategies, which integrate the information on the system's health state into the control loop of the process, have shown that lifetime improvements can be achieved with some compromise in operation [4]. In this context, some of these approaches propose addressing the Remaining Useful Life (RUL) [5], a key metric for evaluating a system's health and reliability commonly utilized in Prognostic and Health Management (PHM). In particular, RUL provides insights into the system's health status over time by predicting potential failure times [6]. This predictive capability of anticipating potential failures with a probability distribution enables informed decision-making for maintenance actions or operational adjustments, such as reconfiguring the control system tuning to mitigate stress and extend system lifespan [7]. For example, Obando et al. [8] proposed a re-configurable control law to effectively manage RUL in a friction system, while Thuillier et al. [9] suggested incorporating a degradation model into control design to guide the system's lifetime towards desired values. A combination of strategies for extending wind turbine lifespan, mainly focusing on blade control, is explored in Kipchirchir et al. [10].

Despite advances towards re-configurable control based on health specifications and lifespan control, formulating health management as a generalizable control problem remains challenging [5, 11]. In this study, we propose a RUL control problem formulation and a generalizable control framework to be implemented across various applications. To accomplish this, we explore a multi-level control strategy where the primary control focuses on manipulating variables inherent to the process, and the secondary control, which operates with slower dynamics, reconfigures the primary control to manage its lifespan. This approach can also help to alleviate real-time constraints—one of the challenges associated with health management.

Another challenge in health management strategies is degradation modeling, as numerous factors influence its dynamics, and it can be difficult to model it as a function of process variables [11]. As a result, degradation models are commonly tailored to the application or rely on rule-based control strategies. Alternatively, researchers often approach degradation using stochastic theory to simplify the intricate interactions and random processes involved. However, formulating control problems using stochastic models can be difficult. One of the notable attempts can be found in Langeron et al. [7]. We propose an alternative perspective that still regards degradation as a stochastic phenomenon characterized by uncertainties while also exhibiting **controllable** deterministic average behavior. Specifically, in RUL control, where uncertainty is inherent, we aim to iteratively adjust the median of this probabilistic variable to influence the expected End-of-Life (EoL) through real-time decision-making. This is achieved through a re-configurable control law that corrects for potential deviations in the degradation trajectory resulting from interaction with exogenous factors, which are considered components of uncertainty in this behavior. Despite its stochastic nature, we explore how to represent degradation dynamics in a state-space format closely linked to system operation, particularly focusing on linear and exponential trajectories. We aim to establish the relationship between degradation process states—such as the degradation rate influencing the trajectory—and manipulable variables at the operational control level in a particular form of **link function**. Using this formulation, we can design a control law to adjust the operational controls to meet RUL objectives. At this stage, we propose implementing robust control design approaches to ensure stability while addressing the uncertainties present in the modeling.

To demonstrate the practicality of such an approach, we propose implementing it in a Horizontal-axis Wind Turbine (HAWT) with variable speed control, focusing specifically on the drivetrain system. This system features a flexible shaft susceptible to torsional effects, which can result in energy losses. This setup provides an ideal scenario for examining how the proposed control strategy can control the RUL of critical components within controlled systems. By integrating robust control principles into the RUL control problem, we aim to overcome the possible challenges of managing degradation while achieving effective lifetime control. In summary, the main contributions of this article include the following:

1. Formulation of the RUL control problem within the context of controlled systems.
2. Proposition of a generalizable RUL control design framework based on a state-space approach incorporating a re-configurable control law. Solving the control problem involves tracking a desired RUL characteristic target (e.g., the mean or median) of a given RUL probability distribution using a robust control design.
3. Implementation of the approach in a case study, along with the presentation of results that illustrate the benefits of using RUL re-configurable control as a decision-making strategy for adapting standard control laws in controlled systems.

The article is organized as follows: Section 2 presents an application example to provide context and highlight the motivations for an RUL control solution. Section 3 formulates the RUL control problem and explores how to represent the dynamics of the degradation process. Section 4 describes the proposed control approach and framework as a solution to the formulated problem while presenting a robust solution design. Section 5 presents the results of implementing this approach in the motivating case study, along with explicit design details. Finally, Section 6 highlights the study's main findings and suggests potential future research.

2 | Motivating Example: Flexible-Shaft Wind Turbine

This section presents an application that could benefit from the implementation of an RUL controller. We will describe the process control and degradation aspects to further define the RUL control problem based on this investigation.

2.1 | Basic Concepts of a Variable-Speed HAWT

Wind turbines play a crucial role in sustainable energy production. Among the commercially available wind turbines, the variable-speed HAWT is widely used in the energy sector. These HAWTs can adapt according to the wind speed by controlling the rotor speed, allowing them to achieve a desired level of power generation efficiency [12]. The power generated depends on factors such as wind speed (v), air density (ρ_v), swept rotor area (A_r) and energy conversion efficiency (C_p), which is expressed as follows:

$$P_r(t) = \frac{1}{2}\rho_v A_r v^3(t) C_p(\lambda(t), \phi(t)) \tag{1}$$

where C_p represents the percentage of available wind energy (P_{wind}) converted into kinetic energy (P_r), calculated by:

$$C_p(\lambda(t), \phi(t)) = \frac{P_r(t)}{P_{wind}(t)} \tag{2}$$

The variation of C_p depends on both the design of the turbine and process variables, such as the blade angle ($\phi(t)$) and the Tip-Speed Ratio (TSR), denoted as $\lambda(t)$. The combination of blade angle and TSR corresponds to various operational conditions, with the resulting power coefficient (C_p) summarized in the turbine's efficiency curve, for instance, as depicted in Figure 1 for a 5MW HAWT.

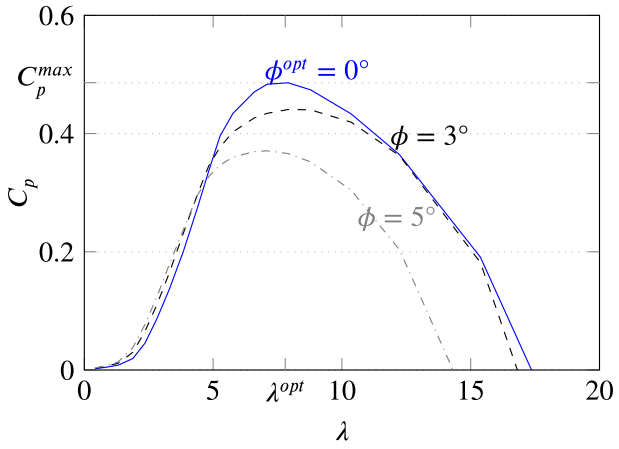

FIGURE 1 | $C_p(\lambda)$ curves of NREL 5-MW turbine [13] for different pitch angles ϕ.

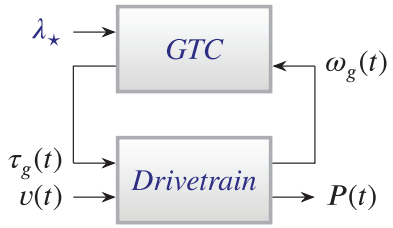

FIGURE 2 | Scheme of a standard generator torque control (GTC).

The TSR represents the relationship between the swept rotor speed (a product of rotational speed, $\omega_r(t)$, and rotor radius, R_r) and the wind speed, $v(t)$, defined by:

$$\lambda(t) = \frac{\omega_r(t) R_r}{v(t)} \tag{3}$$

An optimal combination of parameters (λ^{opt}, ϕ^{opt}) results in the maximum coefficient of efficiency C_p^{max}. In HAWT systems, especially when wind speed is insufficient to produce the rated power, a rotor speed control system is activated to ensure that the TSR remains at the optimal value (λ^{opt}) and that maximum efficiency is achieved ($C_p(t) = C_p^{max}$) while keeping the blade angle constant. This control mechanism, depicted in Figure 2 and referred to as Generator Torque Control (GTC), is responsible for regulating the rotational speed (ω_r), maintaining the TSR at the desired value $\lambda_\star$.

The GTC applies torque that drives the rotation of the transmission shaft, which connects the rotor to the generator components, according to the selected control approach. In the realm of industrial variable-speed HAWTs, a commonly used control strategy (see for instance Johnson et al. [14]), the torque control law is expressed mathematically as follows:

$$\tau_g(t) = K_{mppt}(\lambda_\star) \cdot \omega_g(t)^2 \tag{4}$$

where ω_g denotes the observed rotation speed on the generator side and K_{mppt} represents the *control gain, which is tuned based on the TSR desired value* $\lambda_\star$. Specifically, this control law aims to ensure the equality $C_p(\lambda(t)) = \mathcal{F}(\lambda_\star, \lambda(t))$, where $\mathcal{F}(\lambda_\star, \lambda(t))$ is

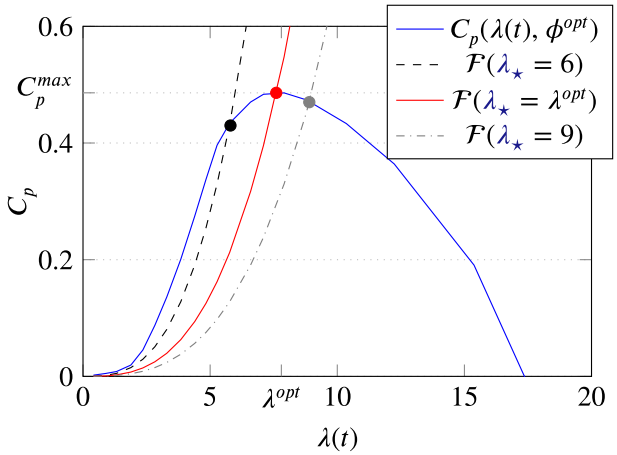

FIGURE 3 | Operating points ($C_p(\lambda) = \mathcal{F}(\lambda)$) for different values of $\lambda_\star$ and $\phi = \phi^{opt}$.

defined as a function of $\lambda(t)$ and its desired value $\lambda_\star$, given by:

$$\mathcal{F}(\lambda(t)) = \frac{C_p(\lambda_\star)}{\lambda_\star^3} \lambda(t)^3 \tag{5}$$

Figure 3 illustrates the $C_p(\lambda)$ curve for different combinations (λ, ϕ) and their respective operating points, i.e., the points where Equation (5) intersects the C_p curve, dictated by the choices of $\lambda_\star$. Typically, GTC selects the operating point $\lambda_\star = \lambda^{opt}$ to maximize power conversion efficiency, ensuring that $C_p(\lambda(t)) = C_p^{max}$. This control design is commonly referred to as Maximum Power Point Tracking (MPPT) [15].

2.2 | Proposed Changes for a RUL Control-Based GTC

The HAWT system exemplifies controlled systems experiencing degradation during operation. Despite its capacity for electricity generation, it encounters structural loads that stress its components, resulting in degradation over time, which in turn diminishes energy production performance and increases failure risks. The intensity of these structural loads depends on both the operational conditions, such as wind conditions, and the control actions [16]. In Romero et al. [17], the authors demonstrated that while controllers aim to track the maximum effective operating point, their corrections may inadvertently increase stress on transmission components. In their experience, the choice of the GTC control gain (K_{mppt}) influences the level of torsional loads in rotation parts, considering a variable-speed HAWT with a flexible shaft. Despite optimized control actions, the MPPT approach does not consider the structural loads endured by the turbine, such as torsional displacements of the wind turbine shaft. These torsional displacements result from the relative difference between the rotor's rotational speed and the generator's rotational speed, calculated as:

$$\tilde{\omega} = \omega_g - \omega_r \tag{6}$$

Selecting higher values for control gain K_{mppt} results in greater levels of relative difference, meaning that operating the GTC at a slightly lower maximum efficiency can reduce loads.

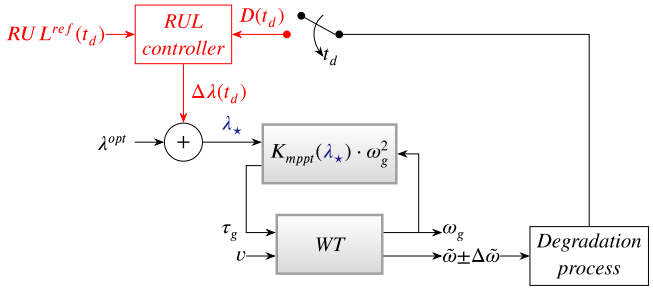

FIGURE 4 | Adaptation of $\lambda_\star$ through a RUL-controller for a controlled wind turbine in the presence of torsional stress.

Consequently, profitability can significantly increase over time due to lower failure rates and reduced repair costs. Of course, the necessary production levels to meet operational requirements will constrain such profit. Finding an **optimal balance** can lead to a production level that meets requirements while minimizing maintenance costs.

To solve this problem, we propose a control strategy illustrated in Figure 4. In this approach, a second-level controller, referred to as **RUL-controller**, calculates the variations of the operating point ($\Delta\lambda$) to decrease (or increase) stress loads ($\tilde{\omega} \pm \Delta\tilde{\omega}$) to track a desired RUL. With this approach, the GTC control law dynamically adjusts the control gain K_{mppt} based on a desired rate in the degradation process. For example, the operating point determined by K_{mppt}, as a function of $\lambda_\star$ can be *iteratively* adjusted by the RUL controller to either accelerate or slow down the nominal degradation process. To guarantee that these corrections stay around the optimal efficiency, we propose to calculate the operation condition adjustment around the optimum point as follows:

$$\lambda_\star(t) = \lambda^{opt} + \Delta\lambda(D(t_d), RUL^{ref}(t_d)) \tag{7}$$

where $\Delta\lambda$ represents a small deviation from the nominal (also optimal) TSR. This deviation should depend, of course, on the current degradation already experienced ($D(t_d)$), and the desired RUL, the so-called RUL, ($RUL^{ref}(t_d)$). Furthermore, the time-step of RUL-controller decision-making t_d should be greater than the time-step of the GTC operation as the degradation has a much slower dynamic than HAWT control operation.

With this approach, the rotation is still controlled with the same control law (given by Equation 4), with an additional adjustment of the control gain parameter. The **stability of the torque control is guaranteed even with different values of** K_{mppt} as long as the operating point remains within the range of the efficiency curve [14]. Such a strategy of RUL control aims to regulate the load associated with the control law—either by reducing or increasing it—without eliminating it while maintaining operation near the nominal point.

These adjustments might reduce the efficiency of a wind turbine's performance in terms of electricity production, but they meet reliability requirements. While this presents a short-term drawback, it can prove advantageous in the long run if these adjustments prolong operational duration while enabling operation near rated power [18]. In essence, *an optimal adjustment manages the lifetime to meet reliability criteria while avoiding* ***unnecessary*** *efficiency losses.*

Motivated by this application example, the design of the RUL-controller solution will be presented in the following sections. While the motivation stems from a specific application, our focus lies on developing a generalizable approach to be implemented in the control loops of different controlled systems that degrade over time during operation.

3 | Problem Statement

In this section, we present the formulation of the RUL control problem by examining the relationship between degradation modeling and process control. Through this examination, we propose a method for RUL control utilizing established control theory approaches.

3.1 | Degradation Process for Control Decision

Designing an optimal control solution requires establishing a dynamic model representing the process to be controlled as a function of the control inputs [19]. However, degradation is influenced by various factors, depends on many often unknown variables and parameters, and typically evolves more slowly than the system's operation dynamics. When trying to model the degradation of a system using physics-based models, various complex models are proposed [11]. These **models pose an additional challenge in implementing control solutions** and often lead to specific solutions for each application. Another approach to modeling degradation is stochastic modeling [7, 20, 21]. These works use historical data to describe an expected behavior, and their advantages are their reduced need for physical information and their ability to include uncertainty properties. The disadvantages are that they still have some degree of complexity, and the integration into control design is not straightforward. Also, they are typically followed by the perspective of maintenance decisions and thus are usually designed to have a good prediction accuracy.

In this context, we propose investigating a more generalized formulation of the degradation phenomena to reduce modeling complexity. While still effectively aiming to capture the phenomenon's random characteristics, it also aims to represent degradation as a function of deterministic process variables, allowing easy integration into the control design.

3.1.1 | Degradation Process Model

In reliability theory, degradation is considered a stochastic phenomenon, meaning it is a function of time and its inherent randomness [1]. A stochastic process can be modeled using a Stochastic Differential Equation (SDE), which is a generalization of the Ordinary Differential Equation (ODE), a more standard format for modeling system behavior and designing control laws. While an ODE typically exhibits deterministic behavior, an SDE can produce different trajectories even with the same initial conditions.

Let us assume that the degradation dynamics follow the differential equation:

$$\frac{dD}{dt} = \beta_1(t)D + \beta_0(t) \tag{8}$$

which express the degradation-rate as a function of the parameters $\beta_1(t)$ and $\beta_0(t)$, represented as a vector $\beta(t) = [\beta_1(t), \beta_0(t)]$. The vector $\beta(t)$ dictates the degradation curve. If $\beta(t)$ is treated as a stochastic process (e.g., if $\beta_0(t)$ is considered as white noise random phenomena), then Equation (8) represents a particular case of an SDE model, such as Wiener or Gamma processes [1], which are often used in reliability and maintenance studies because they are valuable for modeling complex systems with random behavior. In particular, we consider $\beta(t)$ as a generalization of a variable that captures element-to-element variability with a specific a priori probability distribution consistent with the nature of the degradation process. This consideration assumes heterogeneity in degradation pathways commonly observed in the degradation of components, where the same type of component in the same system can have different EoL distributions due to unique properties, such as different internal resistances or strain constants, resulting in different degradation trajectories. This specificity is expressed in the model by $\beta(t)$ with different distribution values.

Although the degradation process has a unique trajectory, its behavior can be generalized by trend models that represent typical trajectories, including linear, exponential, and logarithmic behaviors [1]. Each trend model reflects a different nature of the degradation process. By exclusively selecting β_1 or β_0, we can distinguish between exponential and linear degradation behaviors, respectively. These behaviors are commonly employed to represent damage accumulation within a system. For example, the linear trend can effectively model the wear mechanisms resulting from surface contact, as presented in Reference [22]. In this case, the wear rate is represented by a linear model:

$$\dot{D} = \beta_0(t) \tag{9}$$

where the rate $\beta_0(t) = f(s(t), \tilde{v}(t))$ is influenced by physical variables. Specifically, in this context, these variables are the dynamic load $s(t)$ and the sliding speed $\tilde{v}(t)$ of the contact. An exponential behavior is used to model cumulative degradation processes (e.g., crack propagation), especially in bearing applications. Such behavior can be expressed as follows:

$$\dot{D} = \beta_1(t)D \tag{10}$$

where the trajectory is dictated by $\beta_1(t)$. Similar to $\beta_0(t)$, $\beta_1(t)$ is a time-parameter varying parameter resulting from the interactions of fatigue and process variables.

3.1.2 | Definition of Link Function

Although the values of $\beta(t)$ depend on physical interactions, identifying a degradation model as a function of physical variables is challenging. Consequently, modeling $\beta(t)$ through stochastic behavior is common, relying on historical data for identification. However, these models often lack a clear connection to physical inputs or underlying mechanisms. In contrast, in control theory, explicit physical input-output models are more common because they inherently exhibit input-based behavior tied to control decisions, thus making them more compatible with control design, even in the presence of uncertainties. Specifically, in such models, degradation behavior **explicitly** results from controlled operating conditions.

In this work, we depart from conventional approaches. Specifically, we assume that, although $\beta(t)$ exhibits stochastic behavior, it is possible to identify a function that represents its **average behavior** as a function of a set of available manipulable variables. In particular, regardless of the dispersion characteristics of the vector $\beta(t)$, we assume that its median values are governed by a set of inputs $\mathbf{w}(t)$ that we can control. Moreover, we assume that the parameter vector $\beta(t)$ can be expressed as a function of the input $\mathbf{w}(t)$ using a **monotonic nonlinear function** $f(\mathbf{w}(t))$. This function incorporates the uncertainties by representing potential additive perturbations η and uncertain multiplicative parameters γ, as follows:

$$\beta(t) = \gamma f(\mathbf{w}(t)) + \eta \tag{11}$$

Equation (11) represents what we define as a "**link function**". Essentially, the function $f(\mathbf{w}(t))$ is grounded in the relationship between the manipulable process variables $\mathbf{w}(t)$ and the degradation-rate parameter $\beta(t)$. Naturally, this relationship depends on the complexity of the system dynamics, which can be nonlinear or non-direct. However, in the absence of an explicit degradation model, where the dynamics of the process states are derived from an explicit link function, we assume the existence of a meta-model. A meta-model is an abstraction of real-world phenomena with a mathematical relationship or algorithm representing input and output. The formulation presented in Equation (11) can thus be seen as an approximation, made for control design purposes, of the values of the degradation-rate parameter as a function of inputs of $\mathbf{w}(t)$. The uncertain or random behavior of these dynamics is captured by the uncertainty parameters γ and η. These parameters encapsulate the influence of various operating points or exogenous inputs, which are random and can be represented by a probability distribution.

To illustrate the relationship between the link function and degradation trajectories, Figure 5 shows various realizations of degradation trajectories for both linear and exponential degradation behaviors considering $\beta(t) = \gamma + \eta(t)$ (i.e., $f(\mathbf{w}(t)) = 1$). They result from a combination of item-to-item variability in γ and sample-wise variability in η, both following a normal distribution $(\gamma, \eta) \sim \mathcal{N}(2, 0.5)$. Additionally, Figure 5 also shows the resulting distribution of the hitting time of these realizations, where the median of such a distribution corresponds to the hitting time of the median degradation trajectory (when $\beta(t) = \overline{\beta}$). In other words, the median hitting time is determined by the median degradation behavior, regardless of the specific nature of the degradation process (linear or exponential in these cases).

Based on these findings and under the simplifying assumption that $\mathbf{w}(t)$ can be directly controlled, we propose to act on the average behavior of $\beta(t)$, by making decisions on the value of $\mathbf{w}(t)$, denoted by $\mathbf{w}^d$. It is expected that the distribution of $\beta(t)$ consistently exhibits a monotonic behavior with respect to $\mathbf{w}^d(t)$. In practice, the considered degradation takes place in a controlled

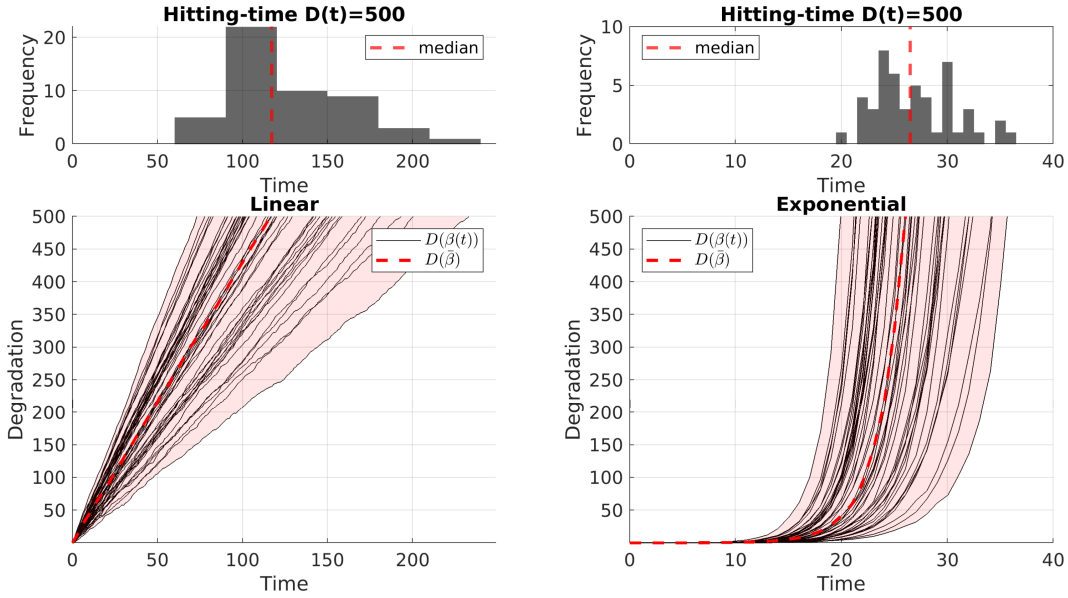

FIGURE 5 | Realizations of degradation trajectories for exponential and linear trends with parameters $(\gamma, \eta) \sim \mathcal{N}(2, 0.5)$ and $f(\mathbf{w}(t)) = 1$. Here, γ varies for each trajectory and η for each sample within a given trajectory. The histograms represent the empirical hitting-time distribution for the value 500.

system; i.e., $\mathbf{w}(t)$ may be different from the control inputs, usually expressed by $u(t)$, whose purpose is to make the system accomplish operational tasks according to operating requirements. Variable $\mathbf{w}(t)$ could represent a parameter of the control law, a reference variable, or another manipulable variable that is often assumed constant in models describing the controlled process. For instance, in the motivating example, $\mathbf{w}(t)$ is equivalent to $\lambda(t)$, a process variable that determines the control law, and the control input is the generator torque $\tau_g(t)$.

Furthermore, the decisions $\mathbf{w}^d(t)$ may not be perfectly integrated into the process dynamics at a given time t, potentially resulting in delays Δt. Given these considerations, we propose to characterize the behavior of $\beta(t)$ by a time-delay relationship:

$$\beta(t + \Delta t) = \gamma f\left(\mathbf{w}^d(t)\right) + \eta \tag{12}$$

For each application or variable chosen to represent $\beta(t)$ and $\mathbf{w}(t)$, Equation (12) takes on a distinct form, with the values of γ and η depending on specific process variables. Furthermore, it should be emphasized that Equation (12) does not describe the time-to-time dynamics of $\beta(t)$ as a function of input variables, which are stochastic dynamics. Instead, it establishes a fundamental link between the parameter $\beta(t)$, which drives the degradation rate, and a manipulated variable intended to influence the degradation trajectory $\mathbf{w}(t)$. This model provides information about the direction of degradation behavior as a function of decision inputs, which can be valuable for control design. Even if the model is dynamically inaccurate, robust approaches can mitigate the need for precise degradation models while ensuring certain performance properties. To enable the use of this model for designing control laws with robust approaches, we assume that γ and η remain within specified bounds. While the exact value of γ remains unknown and uncertain, its boundaries can be determined given the limits of the degradation phenomenon and its intrinsic nature.

3.2 | RUL Control Problem

In summary, the degradation process can be approached as an inherent aspect of system operation—affected by choices of a manipulable variable $\mathbf{w}$—increasing over time with a certain degradation rate until it reaches a maximum allowable level. In this section, we will formulate the problem of RUL control for this degradation process and propose an approach to find a control solution.

3.2.1 | Formulation of RUL Control Problem

The time at which the degradation reaches a maximum allowable level is referred to as "end-of-life" and denoted as t_f. At this point, the system's condition becomes unacceptable, preventing it from performing its designed functions. Thus, $RUL(t)$ can be defined follows:

Definition 1 (Remaining Useful Life). At any time instant t before the end-of-life ($t < t_f$), the system's RUL is the time interval remaining before the degradation reaches a maximum level (D_{max}), satisfying the equality:

$$D(t + RUL(t)) = D_{max} \tag{13}$$

Degradation is a random phenomenon, i.e., there may be several potential degradation paths, each leading to different possible $RUL(t)$ values at any given time t. Therefore, $RUL(t)$ can be represented by a distribution of values—a widely adopted approach in reliability engineering [6]. Alternatively, $RUL(t)$ can be represented by a specific characteristic of this distribution (e.g., the median), which is denoted here $\overline{RUL}(t)$. This representation implies that $\overline{RUL}(t)$ does not necessarily predict the precise "end-of-life", t_f, but instead provides an estimate of the expected

value of t_f, which can be used as a **reference point** for control decisions. In the context of a control tracking problem, these control decisions aim to ensure that the $\overline{RUL}(t) = RUL^{ref}(t)$ follows a reference value $RUL^{ref}(t)$, thereby maintaining the system's operational state for the desired expected duration. Such a type of control problem is referred to here as the **RUL control problem** and can be formulated as follows:

Definition 2 (RUL control problem). At each decision time instant t_d before the end-of-life ($t_d < t_f$), given a desired RUL denoted as $RUL^{ref}(t_d)$, we determine desired values of $\mathbf{w}$, denoted $\mathbf{w}^d$, to adjust the predicted RUL, denoted as $\overline{RUL}(t_d)$, in such a way that the degradation D, starting at $D(t_d)$, reaches its maximal allowable value D_{max} at time $t_d + RUL^{ref}(t_d)$ respecting both the degradation dynamics, given by Equation (8), and the degradation-rate parameter, given by Equation (12).

In this formulation, the desired $RUL^{ref}(t_d)$ represents a desired specific characteristic of the RUL distribution (e.g., the median) that can be based on maintenance constraints or operational requirements for the particular degrading system.

Moreover, according to Equation (8), for a given $RUL^{ref}(t_d)$ there is an associated $\beta^{ref}(t_d)$ that leads to the realization of $D(t_d + RUL^{ref}(t_d)) = D_{max}$. Therefore, we propose a strategy that focuses on correction β, instead of adjusting $\overline{RUL}$ directly, through the following control objective:

$$\mathbf{w}^d = \underset{\mathbf{w}}{\operatorname{argmin}} \|\beta^{ref}(t_d) - \beta(t)\| \tag{14}$$

where $\mathbf{w}^d$ is the optimal value for $\mathbf{w}$, which regulates $\beta(t)$ so that it follows the desired β^{ref}.

In this strategy, the degradation-rate parameter ($\beta(t)$) must be corrected so that it varies, following its stochastic behavior, around reference a value ($\beta^{ref}(t_d)$) that accelerates or decelerates the degradation trajectory to achieve a desired lifetime. In particular, we select $\beta^{ref}(t)$ from the possible values of $\beta(t)$ and determined by combining the current degradation level $D(t)$ and the desired remaining useful life $RUL^{ref}(t)$.

3.2.2 | Proposed RUL-Controller Framework

To address the RUL control tracking problem and find values of $\mathbf{w}^d$, we propose a multi-level control framework, as shown in Figure 6. In this framework, the inner closed-loop process results in degradation and performance according to its operation condition (manipulable and exogenous inputs). Based on predefined objectives and the current degradation level, a reconfiguration of such nominal operation can be performed to apply necessary adjustments to readjust the average degradation rate, thereby changing the course of degradation trajectories. This architecture also includes observing the average degradation behavior to estimate the degradation level. Both the observation and reconfiguration are part of what we refer to here as the **RUL-controller**, an optimal decision-making component responsible for **re-configure** the degrading inner-loop controlled process.

The RUL-controller consists of different components designed to perform specific tasks, as illustrated in Figure 6. These components are described below:

1. *Degradation state observer*: This component aims to estimate the current degradation process states, e.g., $\hat{D}(t_d)$ and $\hat{\beta}(t_d)$. For the observer's design, we assume the availability of a dynamical model of degradation, as described in Section 3.1.1, and the available degradation measurements, which can be obtained directly or indirectly through internal process outputs. We also assume that these measurements may include noise or imperfections. The observer focuses on estimating the average behavior of the degradation process.
2. *Degradation-rate controller*: This component aims to calculate the necessary adjustments using the variable $\mathbf{w}^d$ as an actuator to reconfigure the controlled operation, thereby affecting the resulting degradation. Specifically, these adjustments are designed to correct the estimated ensemble of $\hat{\beta}(t_d)$ towards $\beta^{ref}(t_d)$, ensuring to achieve the desired trajectory of degradation. The variable $\mathbf{w}^d$ does not necessarily represent corrections to the inner controller output; it can also pertain to other manipulable process variables, such as inner-loop control parameters or reference values.
3. *Reference converter*: The degradation-rate controller requires a reference value, $\beta^{ref}(t_d)$, at each decision time t_d, corresponding to the desired degradation trajectory. However, the RUL-controller is designed to achieve a specified remaining useful life, RUL^{ref}. Therefore, a reference converter is necessary to compute $\beta^{ref}(t_d)$ at each decision

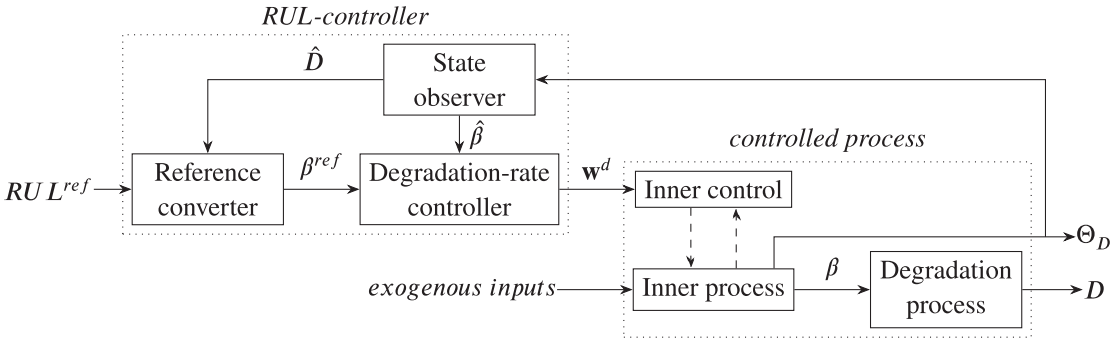

FIGURE 6 | Schematic of a state-space approach for RUL control of a controlled system.

time t_d. This desired degradation rate corresponds to the target $RUL^{ref}(t_d)$ and depends on the estimated current degradation level, $\hat{D}(t_d)$, provided by the state observer, as well as a predefined maximum degradation level, D_{max}.

In this manner, our control objective is to enforce a certain property of the probability distribution of the $RUL(t)$, specifically focusing on the median value, by adjusting $\mathbf{w}^d$. The design of the individual components for this control strategy is detailed in the following sections, based on certain assumptions:

- Degradation can be directly measured or represented by a degradation indicator (Θ_D) estimated from physical measurements.
- Degradation-rate parameter ($\beta(t)$) follows a probability distribution law **with strictly positive values**. The median value of this distribution is governed by the decision variable ($\mathbf{w}(t)$) through a monotonic relationship, as presented in Equation (12). This variable, $\mathbf{w}(t)$, is directly controlled and may incorporate action delays.
- A desired RUL ($RUL^{ref}(t)$) is available at each decision time (t_d). This value is chosen to optimize the trade-off between reliability and performance or be determined based on desired EoL criteria.

4 | Design of the Proposed RUL Controller Framework

In the previous section, we introduced a framework to govern the average behavior of the degradation trajectory by adjusting a process variable, referred to as $\mathbf{w}^d(t)$. In this section, we describe the state-space approach for designing the components of the proposed RUL controller depicted in Figure 6—a state observer, a reference converter, and a degradation-rate controller.

4.1 | Degradation State Observer

Based on Equation (8) and the proposed control strategy, there are two key variables that we aim to estimate for effective control decisions: The current observed degradation level of the system ($\hat{D}(t)$), which is used to determine $\beta^{ref}(t_d)$, and the median behavior of the degradation-rate parameter ($\hat{\beta}(t)$) to be corrected to track the reference. In the presented controller framework, we propose a state observer to estimate these states, represented as $\hat{x}(t) = [\hat{D}(t), \hat{\beta}(t)]^T$, to be estimated online with a state observer.

Several factors, mainly operational behavior, influence the evolution of the degradation process. However, since the EoL aspect is associated with a much longer horizon timescale compared to real-time operations, we suggest focusing on the slower dynamics of this process. Specifically, we emphasize the need to analyze the upward trend of the degradation curve rather than the rapid dynamics, which are more closely related to the decisions made by the inner controller. As discussed in Section 3.1, we can represent these trend behaviors using trend models, whose behavior is particularly influenced by the mean values of the degradation-rate parameter $\beta(t)$. Since Equation (12) does not provide a dynamic representation of $\beta(t)$, we still require a state-based model to capture the temporal dynamics of $\beta(t)$ for the design of the observer. As $\beta(t)$ presents a stochastic behavior, accounting for its random fluctuations (even when influenced by deterministic variables), we propose a general representation of its stochastic behavior using the Langevin equation, as follows:

$$\dot{\beta}(t) = -c\beta(t) + \epsilon \tag{15}$$

which is widely used to model systems influenced by random or fluctuating forces. In this context, c represents an inertia parameter that indicates resistance to change, while ϵ is a noise term representing random effects. The choice of parameter c determines the speed of the expected dynamics. Such an equation avoids the need to explicitly represent $\beta(t)$ as a function of the inner process inputs.

Using these models, we have the state-space matrices necessary for the observer design for the linear and exponential behaviors. For example, in the case of exponential degradation, the observer uses Equations (10) and (15), resulting in the following state-observer estimates:

$$\dot{\hat{x}}(t) = \begin{bmatrix} 0 & \hat{D}(t) \\ 0 & -c \end{bmatrix} \hat{x}(t) + L(y(t) - \hat{D}(t)) \tag{16}$$

where $\hat{x}(t) := [\hat{D}(t), \hat{\beta}(t)]^T$, and L is the correction gain of estimations. Here, it is assumed that real-time estimates of system degradation levels are available. Even if imperfect, health indicators $y(t) := \Theta_D(t)$ can reflect such a system's degradation levels and be derived from direct physical measurements or estimated through more sophisticated algorithms.

The correction gain L is obtained through optimization-based observer approaches. In the example (16), the system exhibits nonlinear behavior. Consequently, the observer proposed must handle nonlinear systems, such as the Linear Parameter-Varying (LPV) observer or the Extended Kalman Filter (EKF). We propose using an LPV formulation for the state observer, solved with a Linear Matrix Inequality (LMI) approach. Details on the synthesis of this observer are provided in further sections.

4.2 | Reference Converter

Instead of explicitly modeling the degradation behavior, we consider the evolution of deterioration as a stochastic process with random effects, represented by an SDE such as Equation (8). The "median solution" for this equation is given by:

$$\overline{D}(t) = D(0) \cdot e^{\overline{\beta}_1 \cdot t} + \overline{\beta}_0 \cdot t \tag{17}$$

where $D(0)$ is the initial degradation value, and $\overline{\beta}_1$ and $\overline{\beta}_0$ are the median values of β_0 and β_1, denoted as $\overline{\beta} := [\overline{\beta_0}, \overline{\beta_1}]$.

Applying this solution at time $t_d < t_f$, we have:

$$\overline{D}(t_d + \overline{RUL}) = D(t_d) e^{\overline{\beta}_1 \cdot \overline{RUL}} + \overline{\beta}_0 \cdot \overline{RUL} \tag{18}$$

where $D(t_d)$ is the "initial" state of the degradation, which also corresponds to the current level assumed to be estimated. If $\overline{\beta}$

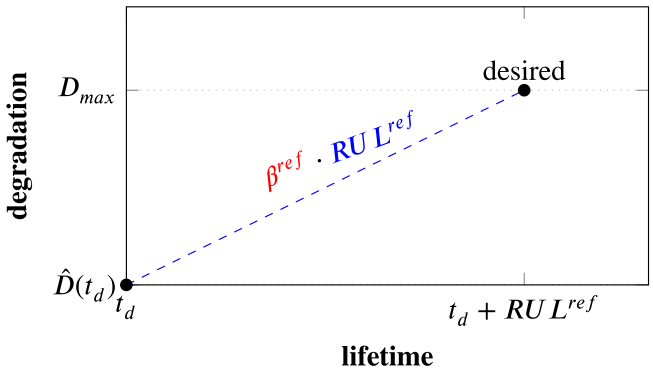

FIGURE 7 | Illustration of median solution $\overline{D}$ at each time decision t_d.

remains constant over time $\overline{RUL}$, then the given solution reaches its maximum value $\overline{D}(t_f) = D_{max}$ at $t_f = t_d + \overline{RUL}$.

Figure 7 illustrates a projected median solution for an arbitrary degradation trajectory, extending from time t_d to $t_d + \overline{RUL}$. This projection assumes that $\overline{\beta}$ remains constant during the interval. The system has been experiencing degradation for $t < t_d$, with decisions made at t_d iteratively based on the sampling schedule and the median solution. At each decision point t_d, a new $\overline{RUL}$ results from the updated degradation level $D(t_d)$.

The Equation (18), $\overline{RUL}$ resulted is a function of the parameters $\overline{\beta}_1$ and $\overline{\beta}_0$. Therefore, for a desired $\overline{RUL} = RUL^{ref}$, there is a corresponding $\beta^{ref} = [\beta_0^{ref} \ \beta_1^{ref}] \in \beta$ vector that enforces the equality $\overline{D}(t_f) = D_{max}$, which can be found by using Equation (18) to solve the problem described below:

$$\beta^{ref} = \underset{\overline{\beta} \in \beta, \overline{RUL} = RUL^{ref}}{minimize} \left| \overline{D}(t_d + \overline{RUL}) - D_{max} \right| \tag{19}$$

The solution to this problem typically requires numerical methods. However, it is also possible to find explicit solutions by separating the degradation dynamic terms in Equation (18) into their exponential and linear trends.

For a linear trend, the degradation median solution reaches D_{max} at:

$$D(t_d) + \overline{\beta_0} \cdot \overline{RUL}(t_d) = D_{max} \tag{20}$$

where $D(t_d)$ is the current degradation state and $\overline{\beta_0}$ is a constant value. Therefore, for a given $\overline{RUL}(t_d) = RUL^{ref}$, there is a β_0^{ref} that guarantees such equality and is calculated as follows:

$$\beta_0^{ref}(t_d) = \frac{1}{RUL^{ref}} \left(D_{max} - \hat{D}(t_d) \right) \tag{21}$$

where $\hat{D}(t_d)$ is the current degradation state estimated by the observer, and the desired $RUL^{min} \leq RUL^{ref} \leq RUL^{max}$ is limited by possible values $\beta_0^{max} \geq \beta_0^{ref} \geq \beta_0^{min}$, which is given by the operating conditions. If an expected lifetime t_f^{ref} is given, RUL^{ref} can be computed at each time t_d using

$$RUL^{ref} = t_f^{ref} - t_d$$

For an exponential trend, the degradation median solution reaches D_{max} at:

$$D(t_d) e^{\overline{\beta_1} \cdot RUL(t_d)} = D_{max} \tag{22}$$

where $D(t_d)$ is the current degradation state and $\overline{\beta_1}$ is a constant value. Thus, the desired parameter β_1^{ref} given a $RUL(t_d) = RUL^{ref}$ is calculated as:

$$\beta_1^{ref}(t_d) = \frac{1}{RUL^{ref}} \ln\left(\frac{D_{max}}{\hat{D}(t_d)} \right) \tag{23}$$

where $\hat{D}(t_d)$ is the current degradation state estimated by the observer.

The Equation (21) or (23) can be used to find references for $\beta^{ref}(t_d)$ for a given RUL^{ref} at each decision moment for the recalculation of $\mathbf{w}^d$. Different assumptions regarding the degradation dynamics may lead to different values of β^{ref}. However, this reference is recalculated at each instance t_d with the updates of observed degradation.

4.3 | Degradation-Rate Controller

The objective of the degradation-rate controller is to find the adjustments of the control system around its nominal behavior to regulate the degradation rate parameter. To do so, we investigated a link function that links the degradation rate and manipulable control parameters. This relationship is often complex and may not be immediately obvious [11]. To account for this, we assume that the parameter β follows the Equation (8), a monotonic relationship with uncertain behavior with respect to a controllable variable $\mathbf{w}$. This behavior is influenced by an uncertain parameter $\gamma > 0$, a normal noise term η, and a one-step delay in decision-making, represented by $\mathbf{w}^d$. Such a model can be represented by a discrete-time form as follows:

$$\mathbf{w}_{k+1} = \mathbf{w}_k^d \tag{24}$$

$$\beta_k = \gamma \cdot f(\mathbf{w}_k) + \eta_k \tag{25}$$

The RUL controller reconfigures the manipulable variable, $\mathbf{w}_k^d$, around its nominal value, $\mathbf{w}_{nom}$, as follows:

$$\mathbf{w}_k^d = \mathbf{w}_{nom} + u_k \tag{26}$$

where u_k is the control input that stabilizes the system described by Equations (24) and (26). Therefore, a more insightful representation of the link function is its linearized form:

$$\beta_k = \beta^{nom} + \Delta\beta_k, \text{where} \tag{27}$$

$$\Delta\beta_k = \overbrace{\tilde{\gamma}\left(\gamma \cdot \frac{\partial f}{\partial \mathbf{w}}\Big|_{\mathbf{w}_{nom}} \right)}^{} \cdot \Delta\mathbf{w} \tag{28}$$

with boundaries of $\tilde{\gamma}_{min} \leq \tilde{\gamma} \leq \tilde{\gamma}_{max}$ predefined by operational conditions. The corrections u_k will not completely prevent the degradation of the controlled system, but they regulate the rate of degradation around the nominal behavior. Although we use

the linearized form to formulate the control problem around the nominal control process, its linearization *not* is necessary for the control synthesis.

The tracking problem we are addressing involves rewriting the RUL control as a problem of tracking a reference value of β^{ref}, which is obtained from the reference converter. To minimize the tracking error, as defined in Equation (14), we propose an integral action z, which accounts for the error between the current value β_k and the reference value β_k^{ref}, as follows:

$$z_{k+1} = z_k + \left(\beta_k - \beta_k^{ref}\right) \tag{29}$$

Finally, the control problem consists of finding a control law that stabilizes the system:

$$x_{k+1} = \begin{bmatrix} 0 & 0 \\ \underbrace{\tilde{\gamma}_k}_{\text{random}} & 1 \end{bmatrix} x_k + \begin{bmatrix} 1 \\ 0 \end{bmatrix} u_k + \begin{bmatrix} 0 \\ -1 \end{bmatrix} \Delta\beta_k^{ref} \tag{30}$$

where $\tilde{\gamma}_k$ represents a random model parameter constrained by the characteristics of the degradation process and operational constraints. The control input u_k can be performed by a state feedback control law $u_k = -Kx_k$. A more interesting realization of this control law will be:

$$u_k = -K_1 \cdot u_{k-1} - K_2 \cdot z_k \tag{31}$$

since it is written in terms of available well-known variables. Remark that only the degradation-rate β_k has to be estimated to perform the full state feedback control law given by (29) and (31). Therefore, the RUL-controller can be implemented by combining the state feedback control law, described by (29) and (31), and a reference generator (or reference converter) function, while considering exponential and/or linear degradation dynamics.

The feedback control gains $K = [K_1\ K_2]$ can be obtained through, for instance, optimal control design techniques, such as H_∞, Robust Control synthesis, or Linear-Quadratic Regulator (LQR) design. The parameter γ can vary within a given interval of possible values resulting in an **uncertain model** within bounded operating conditions. Therefore, a **robust** LQR approach is proposed to consider such uncertainty explicitly. This robust control approach ensures the system maintains stability and performance across the entire range of possible γ values.

4.4 | Description of the Synthesis of a Robust Solution

We aim to address the formulated problem with robust solutions designed to handle model uncertainties effectively. To achieve this, we propose an LPV polytopic approach to implement both the degradation-rate controller and the degradation state observer.

4.4.1 | Definition of an LPV Model Using a Polytopic Approach

Consider the LPV system in a state-space general form, as follows:

$$x_{k+1} = A(\rho_k)x_k + Bu_k + Ew_k \tag{32}$$

where $x_k \in \mathbb{R}^n$ is the state vector, $u_k \in \mathbb{R}^m$ is the control input variable, and $w_k \in \mathbb{R}^n$ is the disturbance input, and $\rho_k \in \mathbb{R}^L$ is a vector of varying parameters.

Assuming all parameter $\rho_k^{(j)} \in [\rho_{min}^{(j)}\ \ \rho_{max}^{(j)}]$, for $j = 1, \ldots, L$, are bounded and known, it can be represented by a convex combination of the $N = 2^L$ vertices $\theta^{(i)} \in \mathbb{R}^L$, for $i = 1, \ldots, N$, of a polytopic set $\Omega_\rho \subset \mathbb{R}^L$ [23], as follows:

$$\rho_k = \sum_{i=1}^{N} \alpha_k^{(i)} \theta^{(i)} \tag{33}$$

where $\alpha_k^{(i)}$ satisfies the conditions $\alpha_k^{(i)} \geq 0$ and $\sum_{i=1}^{N} \alpha_k^{(i)} = 1$.

If the parameter ρ_k appears in an affine form within the matrix $A(\rho_k)$, then the system matrix $A(\rho_k)$, at any operating point $\rho_k \in \Omega_\rho$, can be represented as a convex combination of the Linear Time-Invariant (LTI) system in the $N = 2^L$ vertices of the polytopic region:

$$A(\rho_k) = \left(\sum_{i=1}^{N} \alpha_k^{(i)} A^{(i)}\right) \tag{34}$$

where

$$A^{(i)} := A(\theta^{(i)})$$

are the a priori known system matrices at the extreme values of the convex polytopic set Ω_ρ. The polytopic coordinates α_k are the same as those that appeared in Equation (33).

4.4.2 | Synthesis of a Robust LQR

The LQR approach is an optimal control approach that aims to determine the feedback control $u_k = -\mathbf{K}x_k$ that minimizes a quadratic cost function represented as follows:

$$J = \sum_{k=0}^{\infty} \left(x_k^T Q x_k + u_k^T R u_k\right) = \sum_{k=0}^{\infty} h_k^T h_k \tag{35}$$

where $h_k = \mathbf{M}x_k + \mathbf{N}u_k$ is the energy output of the system to be minimized and $Q = Q^T \succ 0$ and $R = R^T \succ 0$.

The cost function balances control feedback performance with the energy or effort needed to control, penalizing large deviations from desired states and excessive control inputs.

Given a LPV system in the form of Equation (32) and the cost function (35), the optimal gain $\mathbf{K}$ can be found solving the following problem:

$$\min\ trace\left((\mathbf{M} - \mathbf{NK})P(\mathbf{M} - \mathbf{NK})^T\right) \tag{36}$$

$$\text{s.t.:} P \succ 0 \tag{37}$$

$$(A^{(i)} - B\mathbf{K})P(A^{(i)} - B\mathbf{K})^T - P + Q \prec 0,\ \ for\ \ i = 1, \ldots, N \tag{38}$$

where

$$\mathbf{M} = \begin{pmatrix} Q^{1/2} \\ 0_{m,n} \end{pmatrix} \text{ and, } \mathbf{N} = \begin{pmatrix} 0_{n,m} \\ R^{1/2} \end{pmatrix} \tag{39}$$

The conditions expressed in Equations (37) and (38) are known to be necessary and sufficient for u_k to stabilize the system in Equation (32) if they are satisfied for all extreme matrices $A^{(i)}$ describing the polytopic system [24, 25].

Because the system (32) is disturbed by the input w_k with covariance $Q := \mathbb{E}(w_k w_k^T)$, and $\mathbb{E}(w_k) = 0$, we do not have $x_k \to 0$, and then we can expect that the *average* cost function[1] will be:

$$J_{avg} = \lim_{n\to\infty} \frac{1}{n} \sum_{k=1}^{n} h_k^T h_k = \mathbb{E}[h_k^T h_k] = \text{trace}(\mathbb{E}[h_k h_k^T]) \tag{40}$$

where the Hutchinson lemma[2] has been used. Now, the minimization of (40) can be achieved by:

$$\min \text{ trace}\big((\mathbf{M} - \mathbf{NK})P(\mathbf{M} - \mathbf{NK})^T\big) \tag{41}$$

where $P := \mathbb{E}[x_k x_k^T]$, has to verify condition (38) for assuring stability of the closed-loop system.

To address the problem defined by (36–38), we can reformulate it as an LMI problem, as introduced by Boyd et al. [26]. This approach has several advantages, mainly because LMIs are particularly effective in solving convex optimization problems using robust numerical methods. To proceed with this reformulation, consider the condition in Equation (38) to be written as follows:

$$(A^{(i)} - B\mathbf{K})PP^{-1}P(A^{(i)} - B\mathbf{K})^T - P + Q \preceq 0 \tag{42}$$

Applying a Schur complement, the condition becomes:

$$\begin{pmatrix} -P + Q & (A^{(i)}P - B\mathbf{K}P) \\ * & -P \end{pmatrix} \preceq 0 \tag{43}$$

By introducing a change of variables[3], where $\mathbf{Y} := \mathbf{K}P$, the following LMI condition can be derived:

$$\begin{pmatrix} -P + Q & (A^{(i)}P - B\mathbf{Y}) \\ * & -P \end{pmatrix} \preceq 0 \tag{44}$$

In addition, the cost function in Equation (36) can be rewritten by considering an upper bound $W \in \mathbb{R}^{(n+m)\times(n+m)}$, as follows:

$$W - \big((\mathbf{M} - \mathbf{NK})P(\mathbf{M} - \mathbf{NK})^T\big) \succeq 0 \tag{45}$$

equivalently,

$$W - \big((\mathbf{M} - \mathbf{NK})PP^{-1}P(\mathbf{M} - \mathbf{NK})^T\big) \succeq 0 \tag{46}$$

Now, by applying a Schur complement to that condition, we have:

$$\begin{pmatrix} W & (\mathbf{M}P + \mathbf{NY}) \\ * & P \end{pmatrix} \succeq 0 \tag{47}$$

Thus, the LQR problem in its LMI form becomes one of finding W, P, and $\mathbf{Y}$ such that

$$\min \textit{trace}(W) \tag{48}$$

$$P \succ 0 \tag{49}$$

subject to the conditions in Equations (44) and (47), which ensure the stability of the system described by all convex combinations of extreme matrices $A^{(i)}$. Once the problem is solved, the optimal state feedback gain can be computed as $\mathbf{K} = \mathbf{Y}P^{-1}$.

4.4.3 | Synthesis of an LPV Observer

Consider the following estimation error dynamics, represented in a general state-space form of an LPV system:

$$\varepsilon_{k+1} = \big(A(\rho_k) - LC\big)\varepsilon_k \tag{50}$$

where $\varepsilon_k = [x_k - \hat{x}_k] \in \mathbb{R}^n$ is the estimation error vector and $\rho_k \in \mathbb{R}^L$ is a vector of varying parameters.

Since $(A(\rho_k) - LC)^T = (A(\rho_k)^T - C^T L^T)$, we can use the LQR approach to find a matrix gain L that solves the observer design problem. Thus, the cost function to be minimized is similar to that presented in Equation (35), but here $h_k = (\mathbf{M} - \mathbf{N}L^T)\varepsilon_k$. Thus, we are interested in minimizing an estimation error-related cost. That is:

$$\min \text{ trace}\big((\mathbf{M} - \mathbf{N}L^T)P(\mathbf{M} - \mathbf{N}L^T)^T\big) \tag{51}$$

If the matrix system $A(\rho_k)$ has an affine form w.r.t ρ_k, the observer gain L can be obtained as the convex combination of N constant matrices. That is,

$$L = \sum_{i=1}^{N} \alpha_k^{(i)} \mathbf{L}^{(i)} \tag{52}$$

where $\mathbf{L}^{(i)} \in \mathbb{R}^n$ can be found by solving the following optimization problem:

$$\min \textit{trace}\big((\mathbf{M} - \mathbf{NL}^{(i)T})P(\mathbf{M} - \mathbf{NL}^{(i)T})^T\big) \tag{53}$$

$$\text{s.t.:} P \succ 0 \tag{54}$$

$$(A^{(i)} - \mathbf{L}^{(i)}C)^T P(A^{(i)} - \mathbf{L}^{(i)}C) - P + Q \preceq 0, \quad \textit{for} \quad i = 1, \ldots, N \tag{55}$$

where

$$\mathbf{M} = \begin{pmatrix} Q^{1/2} \\ 0_{m,n} \end{pmatrix}, \mathbf{N} \qquad = \begin{pmatrix} 0_{n,m} \\ R^{1/2} \end{pmatrix} \tag{56}$$

Remark that the matrix P satisfying condition (55) for all matrices $A^{(i)}$, $i = 1, \ldots, N$, ensures the stability of the estimation error dynamics (50).

Now, the problem can be solved numerically, in a similar way to that of a robust controller synthesis problem. To do this, the Schur complement is applied to Equation (55), so the condition becomes:

$$\begin{pmatrix} -P + Q & (A^{(i)T}P - C^T\mathbf{L}^{(i)T}P) \\ * & -P \end{pmatrix} \preceq 0 \tag{57}$$

The problem can be simplified by defining a new variable $\mathbf{Y}^{(i)} := (\mathbf{L}^{(i)T} P)$, where a unique matrix P is required so that:

$$\begin{pmatrix} -P + Q & (A^{(i)T} P - C^T \mathbf{Y}^{(i)}) \\ * & -P \end{pmatrix} \preceq 0 \tag{58}$$

In addition, the cost function in Equation (53) with $h_k = (\mathbf{M} - \mathbf{N}\mathbf{L}^{(i)T})\epsilon_k$ can be rewritten as follows, taking into account an upper bound $W \in \mathbb{R}^{(n+m)\times(n+m)}$:

$$W - \left((\mathbf{M} - \mathbf{N}\mathbf{L}^{(i)T}) P (\mathbf{M} - \mathbf{N}\mathbf{L}^{(i)T})^T\right) \succeq 0 \tag{59}$$

equivalently,

$$W - \left((\mathbf{M} - \mathbf{N}\mathbf{L}^{(i)T}) P P^{-1} P (\mathbf{M} - \mathbf{N}\mathbf{L}^{(i)T})^T\right) \succeq 0 \tag{60}$$

If we now apply a Schur complement to this condition, we get:

$$\begin{pmatrix} W & (\mathbf{M}P + \mathbf{N}\mathbf{Y}^{(i)}) \\ * & P \end{pmatrix} \succeq 0 \tag{61}$$

The LQR equivalent problem for solving the observer design problem, in its LMI form, is, therefore, to find W, P, and $\mathbf{Y}^{(i)}$ for every $i = 1, \ldots, N$, such that

$$\min \; trace(W) \tag{62}$$

$$P \succ 0 \tag{63}$$

subject to the conditions (58) and (61). Once the problem is solved, the optimal robust observer gain, at every vertex $i = 1, \ldots, N$, is calculated as $\mathbf{L}^{(i)} = (\mathbf{Y}^{(i)} P^{-1})^T$.

5 | Results: Application on the Motivating Example

In this section, we present the implementation of the proposed approach using the motivating example as a case study. This example aims to demonstrate the effectiveness of the proposed approach for RUL control and highlight the advantages of using RUL control in degrading systems, particularly in a HAWT system. Accordingly, we first present the modeling of a HAWT with a flexible shaft drivetrain subject to torsion, followed by the implementation steps of the RUL controller, including the identified link function. Finally, the simulation results are detailed.

5.1 | Model Description of the HAWT With Flexible-Shaft Drivetrain

To evaluate the effectiveness of the proposed method, we conducted simulations using the wind turbine model from Bianchi et al. [27]. This model represents a HAWT with a flexible shaft drivetrain. The interactions within the model are depicted in Figure 8.

The system represented in Figure 6 is equivalent to the controlled process subject to degradation given the rotation-generated loads, where we would like to interfere with a reconfiguration strategy using RUL-controller.

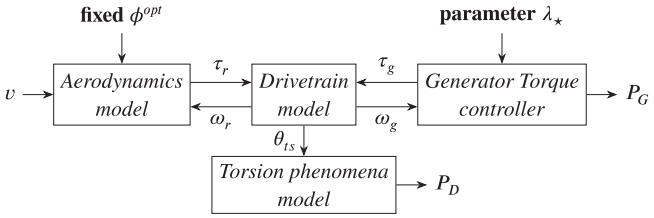

FIGURE 8 | Block diagram of the simulated inner-loop process: Models of the different HAWT components considered.

TABLE 1 | Wind turbine simulation parameter.

Parameter	Description	Value	Unit
$\overline{v}$	Average wind	10	ms^{-1}
$\tilde{v}_{min}$	Minimum wind turbulence intensity	5	ms^{-1}
$\tilde{v}_{max}$	Maximum wind turbulence intensity	0.2	ms^{-1}
ρ_v	Air density	1.225	kgm^{-3}
R_r	Rotor radius	57.5	m
B_{dt}	Damping of the drivetrain	755.49	$Nmsrad^{-1}$
K_{dt}	Stiness of the drivetrain	$2.7 \cdot 10^9$	$Nmrad^{-1}$
J_r	Inertia of the rotor	$55 \cdot 10^6$	kgm^{-2}
J_g	Inertia of the drivetrain	$55 \cdot 10^6$	kgm^{-2}
C_p^{max}	Max. power coefficient	0.486	.
λ^{opt}	Optimal tip-speed ratio	7.6	.
ϕ^{opt}	Optimal pitch angle	0	deg

Source: Extracted from Simani et al. [12].

5.1.1 | Aerodynamics Model

This system is subjected to two forces in opposite directions at different points along the transmission. The first force is τ_r due to the interaction with the wind that reaches the blades and drives their rotation. This force is called aerodynamic torque and can be calculated as:

$$\tau_r(t) = \frac{1}{2}\rho_v A_r \frac{C_p(\lambda(t), \phi(t))}{\omega_r(t)} v(t)^3 \tag{64}$$

Aerodynamic torque $\tau_r(t)$ results from the conversion of the kinetic energy into rotation forces, as shown in Equation (81). The efficiency of such conversion depends on important factors: The current wind speed, the configuration of the blade angles, and the current TSR. The actual efficiency is hardly measured, but it is usually represented by $C_p(\phi, \lambda)$, the output power efficiency coefficient, illustrated by the characteristic curve known as the C_p curve.

In this study, we examine a 4.8 MW HAWT and the corresponding C_p curve is depicted in Figure 1[4]. The parameters of the studied HAWT model are provided in Table 1.

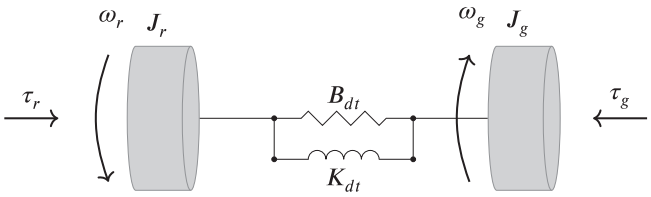

FIGURE 9 | Illustration of two-mass linked by a flexible-shaft drivetrain with dissipation energy phenomena resulting from torsion effects.

5.1.2 | Two-Rigid Bodies Flexible-Shaft Drivetrain Model

As illustrated in Figure 9, the drivetrain is represented by a two-rigid-body system with a flexible-shaft model described by:

$$\begin{bmatrix} \dot{\omega}_r \\ \dot{\omega}_g \\ \dot{\theta}_{ts} \end{bmatrix} = \begin{bmatrix} -\frac{B_{dt}}{J_r} & \frac{B_{dt}}{J_r} & -\frac{K_{dt}}{J_r} \\ \frac{B_{dt}}{J_g} & -\frac{B_{dt}}{J_g} & \frac{K_{dt}}{J_g} \\ 1 & -1 & 0 \end{bmatrix} \begin{bmatrix} \omega_r \\ \omega_g \\ \theta_{ts} \end{bmatrix} + \begin{bmatrix} \frac{1}{J_r} & 0 \\ 0 & -\frac{1}{J_g} \\ 0 & 0 \end{bmatrix} \begin{bmatrix} \tau_r \\ \tau_g \end{bmatrix} \tag{65}$$

where $\omega_r(t), \omega_g(t)$ represents the rotational speed of the rotor side and generator side, respectively, connected by a shaft with torsional dynamics resulting in a torsion angle due to a relative difference speed, denoted $\tilde{\omega}(t) := \dot{\theta}_{ts}(t)$. The model is parameterized by the torsion spring with stiffness K_{dt} and damping B_{dt} coefficients. Such a generator speed $\omega_g(t)$ already accounts for a reduction. If the generator speed is considered without reduction, the actual generator speed can be determined using $\omega_g(t) = \omega_g^{gear}(t)/N_g$, where N_g is the gear ratio and $\omega_g^{gear}(t)$ the speed without reduction.

5.1.3 | Torsion Phenomena and Degradation Model

The torsional phenomena experienced by the system result in structured loads, referred to as "friction forces" [12]. These forces naturally correspond to **energy loss**, as not all potential energy is converted into kinetic energy. The authors propose a dissipation power function that also accounts for losses in the tower and blades; however, we focus only on the drivetrain losses, represented as follows:

$$P_D(t) = B_{dt}(\omega_r(t) - \omega_g(t))^2 \tag{66}$$

We can quantify the system's degradation level using energy dissipation in the friction process [8]. Therefore, we propose using dissipated energy as an indicator of system health[5], which is closely related to the level of degradation caused by torsional loads over time. In particular, we consider the degradation indicator as the cumulative energy dissipated E_D that can be calculated as:

$$E_D(t) = \int P_D(t) \tag{67}$$

which is considered directly proportional to the system's degradation. This estimate assumes that the rotational speeds of both the rotor and generator can be obtained, as indicated by the model presented in Equation (65).

5.1.4 | Generator Torque Controller (GTC)

The second input force is the control torque, which is activated at low wind speeds. This control torque is used to manage the rotational speed to maintain efficiency ($C_p(t) > 0$). The control torque, known as $\tau_g(t)$, is governed by a control law, as described in Equation (4). This law depends on a control gain, K_{mppt}, which is calculated as follows:

$$K_{mppt} = \frac{1}{2}\rho_r A_r R_r^3 \frac{C_p^\star}{\lambda_\star^3} \tag{68}$$

defined by the selected $\lambda_\star$, which determines the desired operating point and its corresponding efficiency, $C_p^\star$. The resulting controller torque regulates the generator speed and electrical power is produced, P_G, which is calculated as follows:

$$P_G = \tau_g \omega_g \tag{69}$$

If the operating point is set to $\lambda_\star = \lambda^{opt}$, the energy conversion efficiency expected is the maximum point $C_p(\lambda(t)) = C_p^{max}$.

5.2 | Design of Proposed RUL Controller

Figure 10 shows the proposed RUL-controller framework's block diagram within the presented HAWT model context. With the established link function in Equation (81), we can implement the proposed control solution for the RUL control problem. The following sections detail the implementation of each component of the RUL controller for this controlled process.

5.2.1 | State Observer

For the observer design, the degradation dynamics are estimated using the following observer equation:

$$\hat{x}_{k+1} = H\hat{x}_k + L(y_k - C\hat{x}_k) \tag{70}$$

where $y_k := E_{Dk}$ is calculated dissipated energy and the estimated states $\hat{x}_k := [\hat{D}_k \ \hat{\beta}_k]$. For the specific case study, the system matrix H and the output matrix C are as follows:

$$H = diag(1,1) + T_s \cdot \begin{bmatrix} 0 & 1 \\ 0 & -c \end{bmatrix}, \quad C = \begin{bmatrix} 1 & 0 \end{bmatrix} \tag{71}$$

defined by the degradation dynamics (15) and (9).

The optimal value of the observer gain L can be found using an LMI solution for the LQ observer problem implemented based on these matrices and the proposed approach in Section 4.4. For the LQ observer problem, we considered:

$$R = 100 \tag{72}$$

assuming noise variances are known and as process noise covariance matrix Q as follows:

$$Q = diag(1, 2.5 \cdot 10^{-5}) \tag{73}$$

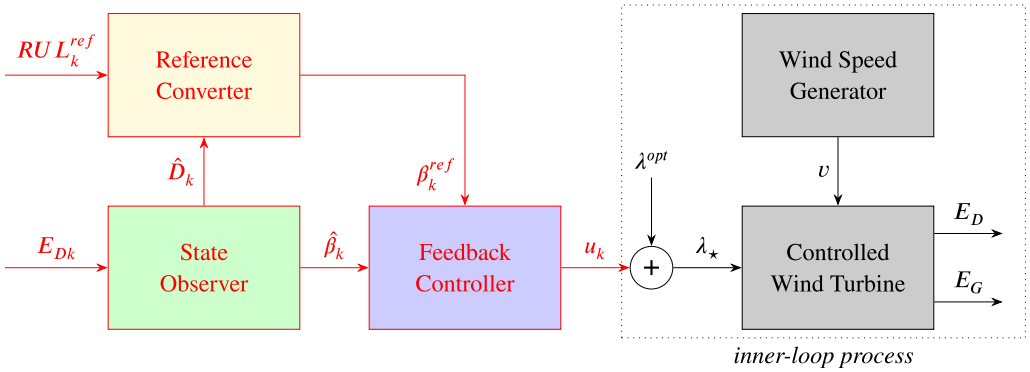

FIGURE 10 | Block diagram of the HAWT system including the RUL-controller components considered for simulation.

Finally, the initial state values were considered:

$$x_0 = \begin{bmatrix} 1 & 10^{-3} \end{bmatrix}^T \tag{74}$$

5.2.2 | Reference Converter

The reference converter serves to calculate the reference of the degradation-rate parameter β^{ref} given RUL criteria RUL_k^{ref}. We assume that degradation D is proportional to the energy dissipation from the torsion effects, which exhibits a **linear** behavior w.r.t P_D. Hence, the reference of the degradation-rate parameter β^{ref} is calculated according to Equation (21) as follows:

$$\beta_k^{ref} = \frac{D_{max} - \hat{D}_k}{RUL_k^{ref}} \tag{75}$$

If an expected lifetime t_f is specified, rather than RUL, then RUL_k^{ref} is calculated as:

$$RUL_k^{ref} = t_f^{ref} - k \tag{76}$$

5.2.3 | Link Function Model Proposition

In the context of a HAWT, the variable dissipated power refers to the degradation-rate parameter, denoted as $\beta := P_D$. As part of the RUL control strategy, we propose adjusting the value of $\lambda_\star$ to regulate the degradation process. Such desired values of the TSR represent the chosen manipulable variable $\mathbf{w}^d := \lambda_\star$. We will need a link function for the control design that captures the monotonic relationship between the selected manipulable process variable and the associated degradation-rate parameter. This relationship can be expressed as follows:

$$P_D = \gamma \cdot f(\lambda_\star) + \eta \tag{77}$$

where γ and η are uncertain elements of the model, and $f(\lambda_\star)$ represents the direct link. Such a link function can be derived from physical modeling or from experimental data. In this study, the link function is obtained by investigating how the interaction between wind and the turbine contributes to energy dissipation due to torsion and how the controlled variable $\lambda_\star$ affects this behavior. For this purpose, let us consider that the wind speed $v(t)$ consists of two components, a static part $\overline{v}$ and a fluctuating part $\tilde{v}(t)$, which characterizes wind turbulence:

$$v(t) = \overline{v} + \tilde{v}(t) \tag{78}$$

When there is no wind turbulence ($\tilde{v} = 0$), the drivetrain controller maintains the angular speed of the shaft at an equilibrium point (eq), with the corresponding equilibrium TSR $\lambda_\star$. At this equilibrium, we have:

$$\omega_{r(eq)} = \omega_{g(eq)} = \frac{\lambda_\star}{R_r}\overline{v} \tag{79}$$

However, in the case of wind turbulence ($\tilde{v}(t) \neq 0$), the system is perturbed, and $\omega_r(t)$ is affected by the current rotor torque ($\omega_r(t) \neq \omega_{r(eq)}$). At this moment, a relative differential velocity is resulted, which we can express as:

$$\omega_r(t) - \omega_{g(eq)} = \frac{\lambda_\star}{R_r}v(t) - \frac{\lambda_\star}{R_r}\overline{v} = \frac{\lambda_\star}{R_r}\tilde{v}(t) \tag{80}$$

Therefore, from Equation (66) and Equations (78–80), at this point ($\omega_r \neq \omega_g$), when the equilibrium is disrupted, we can propose a function that expresses the amplitude and direction of the variations $\beta := P_D$ for different choices $\lambda_\star$, with a monotonic relationship:

$$\beta = \left(\frac{B_{dt}\tilde{v}(t)^2}{R_r^2}\right)\lambda_\star^2 + \eta \tag{81}$$

where $\tilde{v}$ stands for wind turbulence intensity, an exogenous input not directly measured but that can be bounded within $0 < \tilde{v}_{\min} \leq \tilde{v}(t) \leq \tilde{v}_{\max}$, assuming that the wind characteristics, e.g., the maximum gust speed, are known [29]. The dissipated power amplitude also depends on structural factors, such as the parameters R_r and B_{dt}. Lastly, η represents an additive noise parameter of unmodeled dynamics. Here, $\lambda_\star$ assumes the role of the manipulable variable for RUL control, previously referred to as $\mathbf{w}$. Note that for well-functioning angular speed control, $\lambda(t+1) = \lambda_\star$ due to the control system's delay.

5.2.4 | State-Feedback Controller

The objective of the RUL controller is to track the references provided by the reference converter using $\mathbf{w} := \lambda_\star$ as the manipulable decision variable. To achieve this, we propose varying

this parameter around its optimal value, λ^{opt}—the GTC nominal parameter—according to the following:

$$\lambda_{\star k+1} = \lambda^{opt} + u_k \tag{82}$$

where u_k is calculated by the RUL controller using:

$$u_k = -K_1 \cdot u_{k-1} - K_2 \cdot z_k \tag{83}$$

We propose a control law that uses u_k to minimize:

$$z_{k+1} = z_k + \left(\hat{\beta}_k - \beta_k^{ref}\right) \tag{84}$$

where β^{ref} is calculated using (75). Such a control law adjusts λ around the nominal value, which means:

$$\beta(\lambda_\star) = \beta^{nom}(\lambda^{opt}) + \Delta\beta(u) \tag{85}$$

where $\Delta\beta$ is controlled to ensure that the degradation reaches its maximum at the desired remaining time, denoted as RUL_k^{ref}. This approach does not guarantee zero torsion when $\lambda > 0$.

For control design purposes, we can consider the link function from Equation (81) linearized around the nominal value λ^{opt}:

$$\Delta\beta_k = \tilde{\gamma}(t) \cdot \Delta\lambda_{\star k} \tag{86}$$

$$\tilde{\gamma}(t) = \frac{B_{dt}\tilde{v}^2}{R_r^2} 2\lambda^{opt} \tag{87}$$

Using Equations (82), (84–87), we can determine the optimal control gains $K = [K_1, K_2]$ by solving the robust LQR problem as outlined in Section 4.4, and considering the following system:

$$x_{k+1} = \begin{bmatrix} 0 & 0 \\ \tilde{\gamma}_k & 1 \end{bmatrix} x_k + \begin{bmatrix} 1 \\ 0 \end{bmatrix} u_k + \begin{bmatrix} 0 \\ -1 \end{bmatrix} \Delta\beta_k^{ref} \tag{88}$$

where $x_k = [\Delta\lambda_{\star k}\ z_k]$ is the state vector. The parameter $\tilde{\gamma}$ is bounded such that $0 < \tilde{\gamma}_{min} \leq \tilde{\gamma}_k \leq \tilde{\gamma}_{max}$, varying with the possible values of $\tilde{v}_{min} - \tilde{v}_{max}$ based on the selected wind characteristics for simulation. By employing this approach and selecting $Q = diag(1, 1)$ and $R = 10^{-5}$, the calculated control gains are:

$$K_1 = 0.4150,\ K_2 = 0.0093 \tag{89}$$

In practice, the state-feedback controller consists of the implementable Equations (82–84).

5.3 | Simulation Results

In this section, the results of the RUL control problem using a simulation environment are presented.

5.3.1 | Simulation Protocol

Figure 11 describes the simulation environment. The model described in Section 5.1 was implemented along with the designed RUL controller—which includes a reference converter, a degradation states observer, and a degradation-rate controller. The degradation results from the interaction between the HAWT and varying wind speeds, as given by Equations (66) and (67).

The wind speeds are generated using established methods [29] with a random seed, where each seed produces a unique wind speed history with varying turbulence intensities. Consequently, each wind speed curve interacts differently with the HAWT, leading to varied curves of energy degradation (E_D).

We simulate two distinct scenarios:

1. GTC without RUL control where the GTC gain is constant with $K_{mppt}(\lambda_\star = \lambda^{opt})$.
2. GTC with RUL control where K_{mppt} is dynamically adjusted by the RUL controller.

The simulation parameters used in this analysis are outlined in Table 2. The simulations involve two sampling periods: The inner process with $T_{s(inner)} = 1$ s and the RUL controller with $T_{s(outer)} = 10$ s. The expected lifetime (t_f^{ref}) is chosen as 10% greater than the

TABLE 2 | Table of simulation parameters.

Parameter	Description	Value
D_{max}	Maximum acceptable dissipation energy	1000 Ws
$T_{s(inner)}$	Inner process period sampling	1 s
$T_{s(outer)}$	RUL controller period sampling	10 s
t_f^{ref}	Desired lifetime	46.49 h

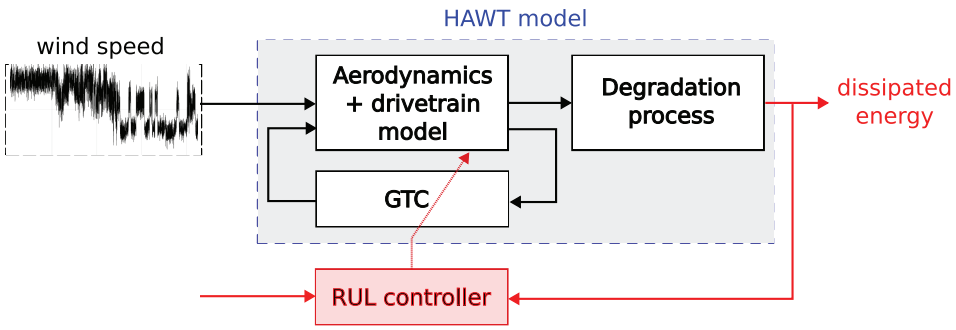

FIGURE 11 | Illustration of the simulation environment.

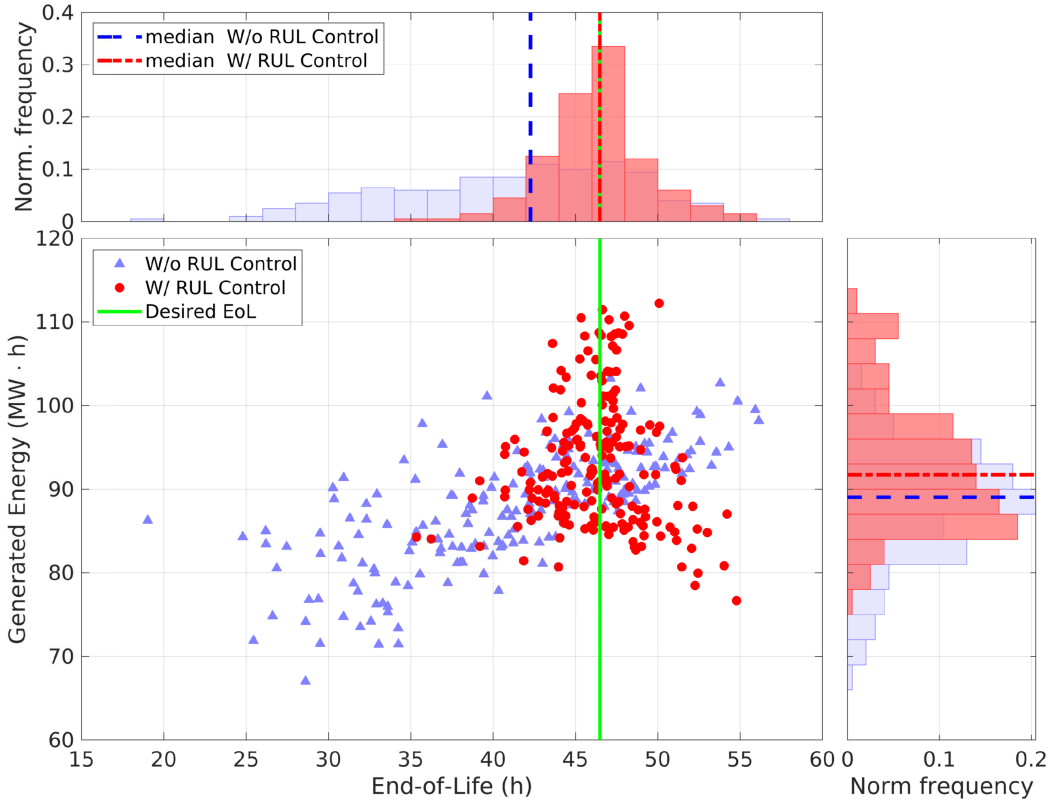

FIGURE 12 | Resulted generated energy and end-of-life for different simulations.

average lifetime of GTC without RUL control. The chosen maximum degradation level (D_{max}) for simulations is intentionally low to enable faster simulation runs. In real-world applications, this value and the corresponding lifetime would be higher.

Using the described model in Section 5.1, the simulation aims to analyze three main aspects:

1. The deteriorating system's EoL and energy generation results from N simulations using different wind speed histories (with varied amplitudes and fluctuations) as input for both GTC scenarios, with and without RUL control.
2. The performance of the state observer and the controller for an arbitrarily chosen wind speed scenario. Assess the quality of the state estimates and the desired degradation-rate corrections in response to wind speed fluctuations while accounting for the undesirable loss of energy efficiency.
3. The total energy produced for different EoL values to explore the relationship between energy production and the choice of t_f^{ref} references. In particular, we aim to investigate the impact of these choices and the limitations of RUL control, especially at large EoL values.

5.3.2 | End-of-Life Vs. Generated Energy

The distribution of the total energy generated as a function of EoL for the $N = 200$ simulation cases is shown in Figure 12. The median and variance of the results for both scenarios are summarized in Table 3.

TABLE 3 | Mean and variance of EoL and total energy for both simulated scenarios.

	End-of-life (h)		Total energy (MWh)	
Scenarios	**Median**	**Std**	**Median**	**Std**
Without RUL control	42.26	7.34	89.03	6.85
With RUL control	46.48 (+10%)	3.06 (−58%)	91.73 (+3%)	8.28 (+20%)

The resulting distribution shows that the scenario without RUL control exhibits a more dispersed EoL distribution than the cases with RUL control. Such dispersion arises from the variability of the wind speed curves. The scenario with the proposed RUL control approach presents the EoL distribution around the desired EoL (t_f^{ref}) (indicated by the green continuous line) and with a lower variance than the GTC without RUL control.

Regarding energy production, the scenario with RUL control resulted in an increase in the average total energy produced, which is expected given the increase in median EoL. The energy production increase was 6.5%, while the EoL increased by 10%. Figure 13 shows the energy generated difference and end-of-life difference when the RUL control is added at each scenario. In most histories, the increase in end-of-life resulted in increased generated energy. Some histories have augmented EoL in 20 h thanks to the RUL control, which also augmented the generated energy.

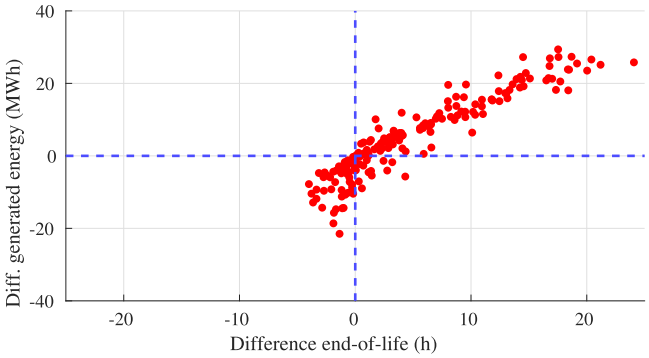

FIGURE 13 | Difference in generated energy and end-of-life (with and without RUL control) for different simulations.

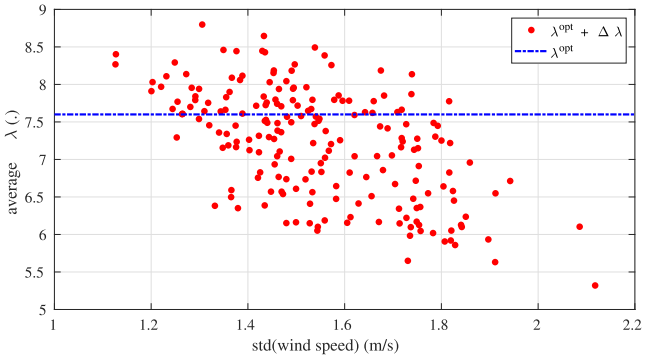

FIGURE 14 | Average λ corrected by RUL control as a function of the standard deviation of the wind speed curve.

On the other hand, some histories extended EoL but did not produce more energy. Additionally, the average increase in generated energy was less than 10%. This lower rate of increase can be explained by the power generation losses incurred while prioritizing the extension of EoL. That is, there is a trade-off between energy production and choices of the RUL reference, leading to reduced efficiency in power production. Despite this trade-off, the improvement could still be beneficial if the resulting EoL distribution significantly reduces O&M costs.

The distribution of λ resulted for different wind speed history is shown in Figure 14, where the resulting average λ decreases according to the wind speed standard deviation. Considering the standard deviation of a wind speed curve as an indicator of turbulence intensity, this result demonstrates the ability of the RUL control to adapt to varying turbulence intensity. Additionally, the variable λ remains close to the optimum value of the MPPT strategy (depicted by the dashed line), which indicates that the GTC with RUL control adjusts the control system's response to accommodate wind speed variations while maintaining power generation close to the nominal operation, as designed.

5.3.3 | Controller and Observer Response for One Wind Speed History

To evaluate the response of the control system for one realization, let us consider an interval of arbitrarily chosen wind speed as shown in Figure 15. The zoom illustrates the variability of the time series of such wind speed, with occurrences of laminar wind (less variance) and turbulent wind (more variance), as well as fluctuations in the average intensity. The HAWT responds differently for each stage of intensity of turbulence.

Figure 16 depicts the system's response for the **entire** wind speed history. It shows the adaptive behavior of K_{mppt} given the corrected values of $\lambda_\star$, aiming to correct the control system response to track the desired RUL. The higher the intensity of turbulences, the higher the torsion, thus lowering expected EoL. The RUL-controller corrects λ to decrease the degradation rate and corrects the expected EoL towards the desired value.

In this wind case, the final EoL value is greater than the desired one, causing a rapid decrease in the control system gain during the last samples. This behavior can be considered undesirable, prompting further investigations to develop a solution that avoids this phenomenon. For instance, update the desired EoL reference once the time surpasses it.

Finally, the final energy produced is higher than in the scenario without RUL control as the HAWT produces longer. However, the energy generation rate is lower with RUL control, by 97.7% of the total final generated power without RUL control in its final sample, clearly demonstrating the impact of changing $\lambda_\star$.

Figure 17a,b display the measurement and estimations of the dissipated energy and power, respectively, of the **zoomed** area of the wind speed. Figure 17c,d present the updates of the degradation-rate parameter references β^{ref} and the output of the RUL controller $\Delta\lambda$. The results show that the proposed observer effectively follows the degradation dynamics, particularly the slow dynamics (more evident in Figure 17a). Meanwhile, the RUL controller compensates for the rapidly increasing dissipation power caused by sudden wind speed changes, as seen, for instance, in the interval around 1.7 h. The adjusted offset of $\Delta\lambda < 0$ guarantees that the dissipated energy reaches its maximum level at the desired EoL, as shown in Figure 16.

5.4 | Energy Production for Different EoL References

Choosing the reference EoL is not straightforward, as the behavior of the control system will also depend on the random behavior of the wind speed and the resulting trade-off is not easy to determine. Here, an analysis is proposed to examine the impact of different references of t_f^{ref} on the result of RUL control.

Figure 18a shows the generated power, and Figure 18b shows the resulting EoL with the RUL control for different EoL choices presented as percentages of the median values of the scenario without RUL control. As expected, the energy production increases in function of the choices of EoL. However, this proportion significantly decreases when it approaches approximately 2 times the nominal EoL, as the **average values of production begin to saturate**. This is explained by the fact that high EoL references might require too large a deviation $\Delta\lambda$ from λ^{opt} to respect the tracking problem, resulting in a loss of efficiency in energy production. Despite the decrease in power generation efficiency, RUL control is consistently efficient across all the

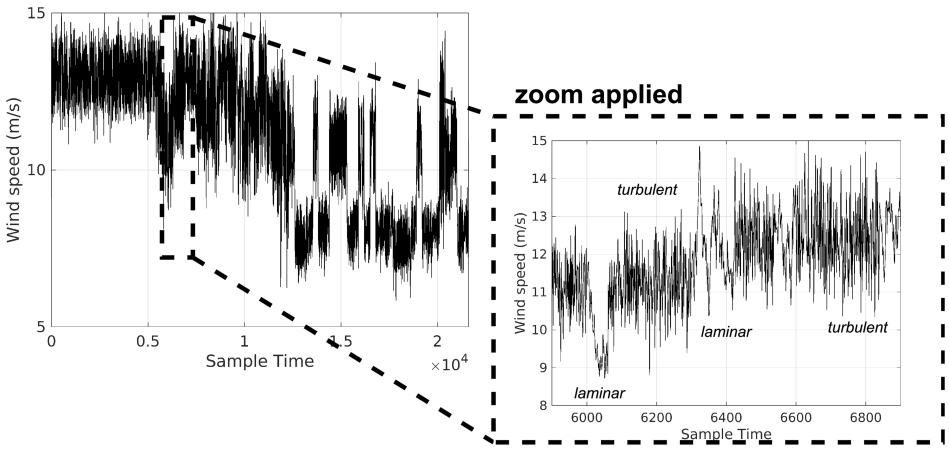

FIGURE 15 | Interval studied of the wind speed curve generated with zoom applied in a specific zone.

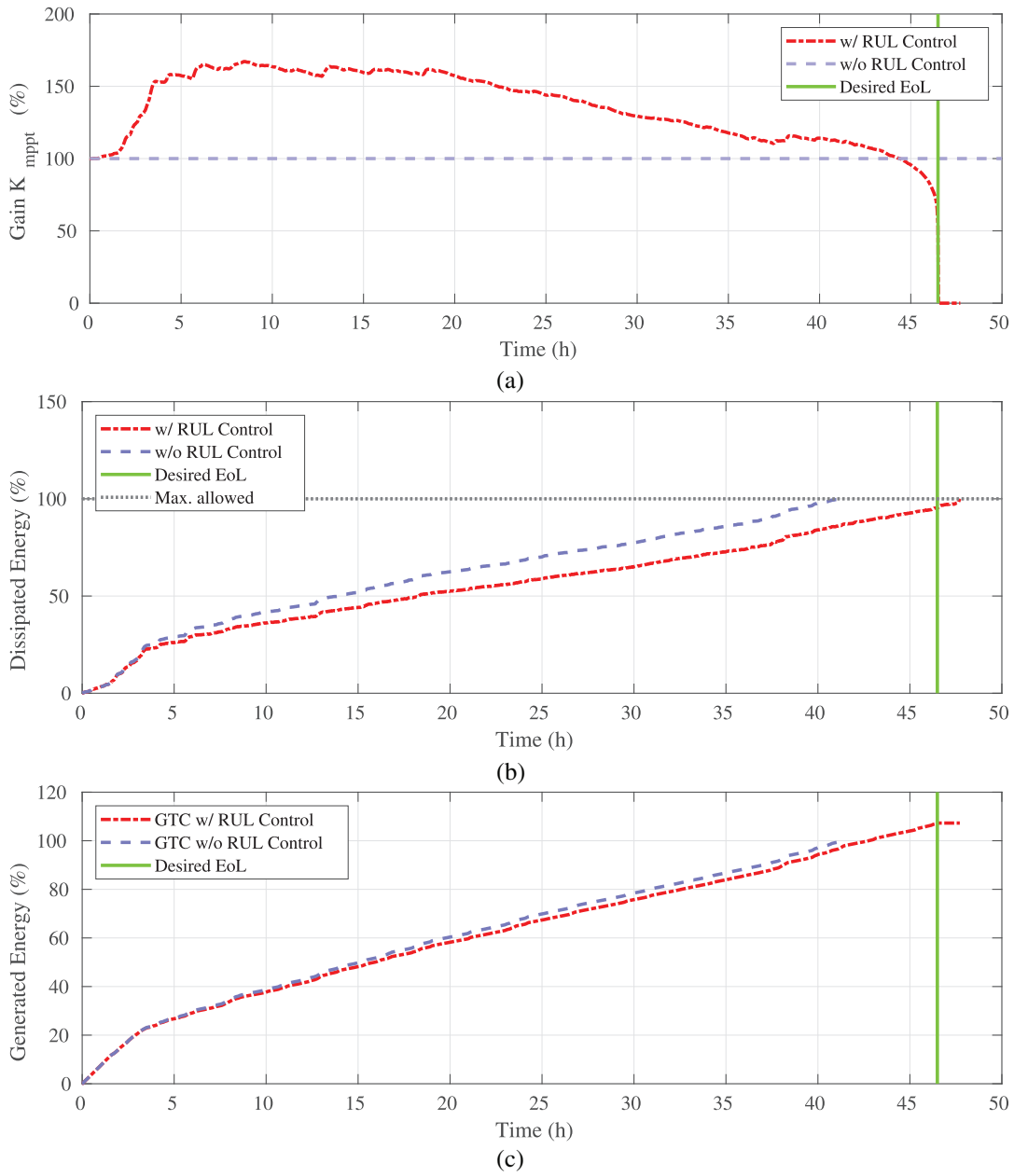

FIGURE 16 | Adaptation of (a) gain values K_{mppt} resulting in a new trajectory of (b) dissipated energy and (c) generated power.

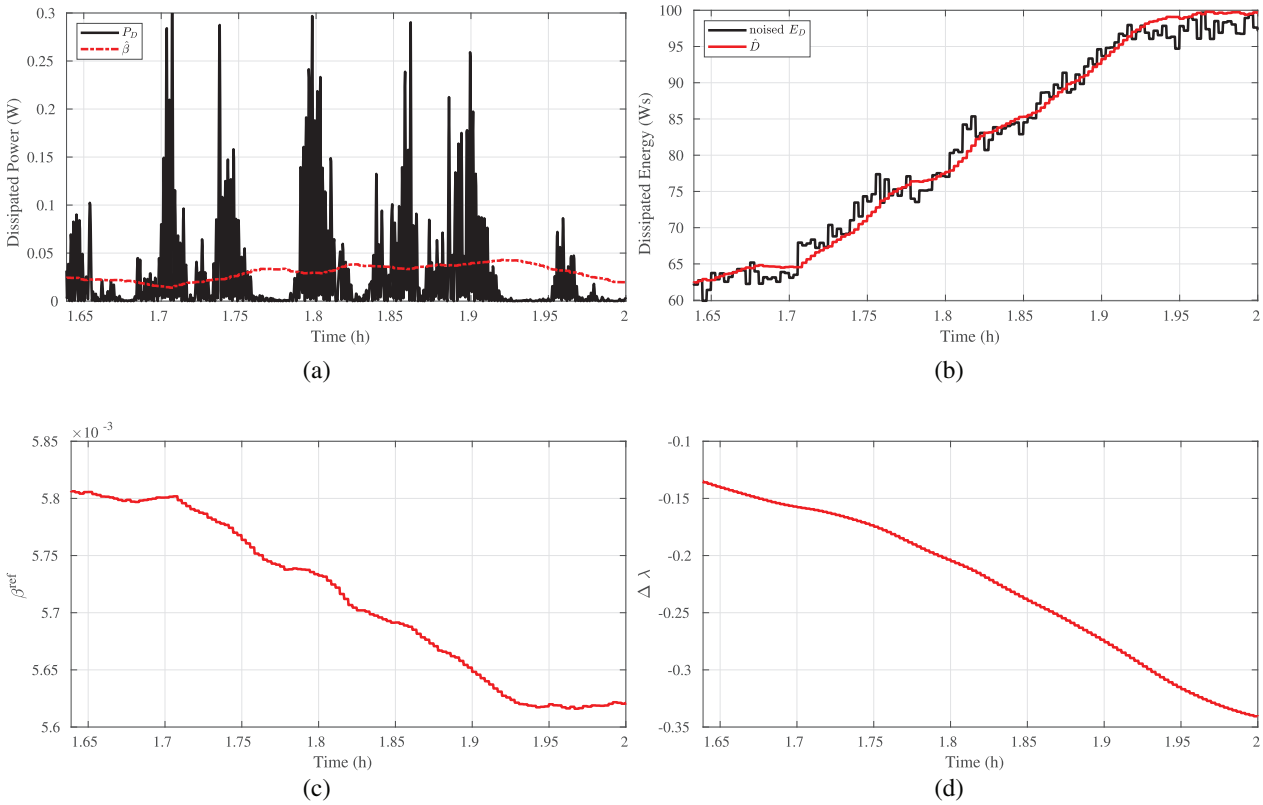

FIGURE 17 | Observer estimation of (a) degradation-rate parameter and (b) degradation level, and controller response with updates of (c) degradation-rate parameter references and (d) $\Delta\lambda$ corrections.

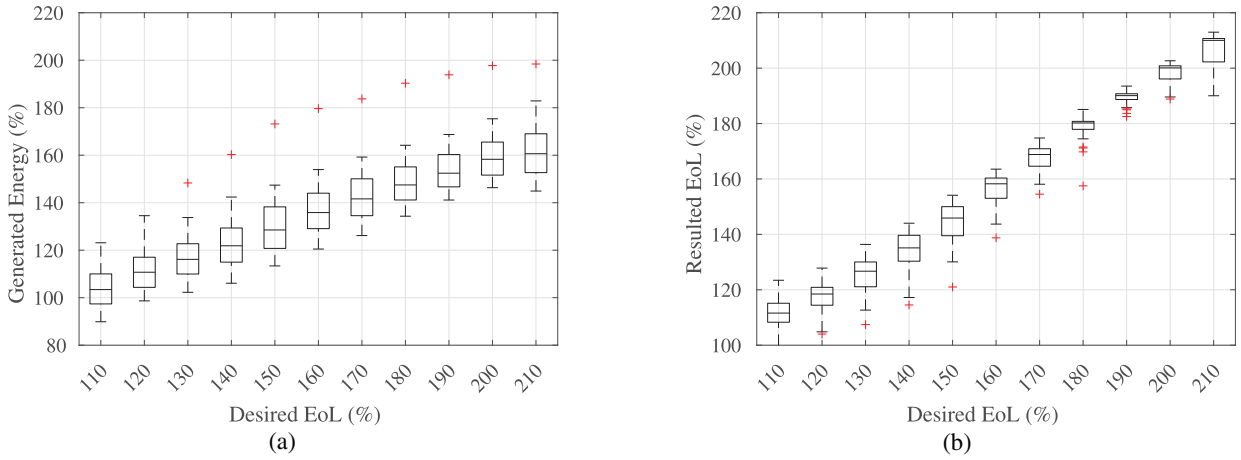

FIGURE 18 | Boxplot representation (with mean and variance values) of the distribution of the resulting (a) generated energy and (b) final EoL (t_f) for different choices of t_f^{ref}.

chosen desired EoL values, showing that the choice of EoL should be based on an optimization task to find an optimized RUL reference, but the RUL controller will effectively assist in the decision-making process.

6 | Conclusion

Recently, the industrial sector has increasingly focused on prognostic and health management as a solution to mitigate unforeseen failures that threaten production, operation, and maintenance resources. RUL estimates have become a crucial parameter for making equipment health-aware decisions, and significant efforts have been put into accurately predicting RUL. Nevertheless, effectively utilizing this predictive information in decision-making processes for equipment lifespan management remains a challenge, highlighting the need to investigate decision-making approaches, including health-aware control methods.

This article presents a method for controlling the RUL of controlled processes. We propose a formulation of the complex task

of controlling a random variable, presenting a solution that reconfigures the process control system according to health criteria. We assume the availability of a manipulable control variable/parameter that affects the degradation rate. By adjusting such a variable around its nominal value, the RUL control objective is to maintain the degradation rate at a desired level so that the expected RUL meets a given reference, accepting some compromises in production output. The proposed RUL control framework focuses on regulating the degradation rate as it is directly linked to possible RUL outcomes. The framework counts with a reference converter that updates the references of a degradation-rate parameter w.r.t. the RUL desired, a state observer to estimate degradation dynamic states, and a controller to calculate the necessary adjustments of the manipulable variable. The state observer employs an LPV approach, while the controller incorporates a state-feedback control law with integral error action and delay action solved with a robust LQR approach. The control strategy ensures that production performance remains acceptable with adjustments made around the nominal control values.

The method can be applied to various controlled processes. This study implements the method in a case study of a variable-speed HAWT with a flexible drive shaft susceptible to torsion, which stresses the device and reduces its lifetime. The key findings when implementing this method to such a case study are as follows:

- The proposed method effectively follows an RUL reference when regulating a degradation-rate parameter directly correlated with the degradation process and the RUL outcomes.
- The proposed state observer consistently estimates the degradation dynamics, providing informed degradation-aware decision-making. The robust LQR problem effectively provides stabilization guarantees around an uncertain model representing the degradation phenomenon.
- Implementing the proposed method ensures that the system will maintain the performance close to its nominal operation while allowing control of the system's RUL.
- The trade-off between production and lifetime output could be optimized through chosen values of the desired f_f^{ref}.

This work offers future perspectives, such as:

- The selection of a desired EoL directly impacts the trade-off associated with balancing production reliability. Therefore, such a choice can be found in solving an optimization problem made by another decision-making level.
- Once this methodology is proposed, it can be applied to other controlled systems, especially where the balance between production and equipment life extension is essential. Potential applications include lithium-ion batteries [30] and other energy systems requiring intelligent health management throughout operational processes.
- This work focused on controlling the expected lifespan of the equipment. Further research could explore controlling other characteristics of the lifespan distribution, which could be crucial in applications where risk management is a key consideration.

This study shows the promising intersection of PHM and control theory domains. It reveals significant advantages of using robust techniques to address the decision-making of random processes, such as degradation. While the link between a process's lifetime and its operation is evident, formulating it into a control problem using known control formulations is challenging. This article aims to contribute to this evolving field and highlight the usefulness of robust control design for addressing these challenges.

Acknowledgments

The authors thank Dr. Marcelo Moratto for the discussions.

Conflicts of Interest

The authors declare no conflicts of interest.

Data Availability Statement

The data that support the findings of this study are available from the corresponding author upon reasonable request.

Endnotes

[1] Considering the fact that $\mathbb{E}[X] = \frac{1}{N}\sum_{i=1}^{N} x_i$.

[2] HUTCHINSON, M. F. 1989. "A stochastic estimator of the trace of the influence matrix for Laplacian smoothing splines". Comm. Stat. Simulat. Comput. 18, 1059–1076.

[3] This transformation simplifies and restructures the problem, making it more computationally tractable.

[4] This curve was derived through regression analysis based on measured data found in Jonkman [13].

[5] Feinberg, A. [28] points out that the degradation process, also known as the aging process, is closely related to the second law of thermodynamics. This law suggests that every system has inherent internal entropy, leading to inefficiency in converting energy into work and energy dissipation. The authors use the term "entropy damage" to describe this process, which directly measures damage or disorder within a system and tends to increase over time.

References

1. M. Rausand, A. Barros, and A. Hoyland, *System Reliability Theory: Models, Statistical Methods, and Applications* 3rd ed., (John Wiley & Sons, 2021).

2. I. El-Thalji and J. P. Liyanage, "On the Operation and Maintenance Practices of Wind Power Asset: A Status Review and Observations," *Journal of Quality in Maintenance Engineering* 18, no. 3 (2012): 232–266.

3. P. Szentannai and T. Fekete, "Integrated Optimization of Process Control and Its Effect on Structural Integrity–A Systematic Review," *Engineering Failure Analysis* 140 (2022): 106101.

4. A. Ray, X. Dai, M. K. Wu, M. Carpino, and C. F. Lorenzo, "Damage-Mitigating Control of a Reusable Rocket Engine," *Journal of Propulsion and Power* 10, no. 2 (1994): 225–234.

5. O. Bougacha and C. Varnier, "Enhancing Decisions in Prognostics and Health Management Framework," *International Journal of Prognostics and Health Management* 11, no. 1 (2020): 1–19.

6. V. Atamuradov, K. Medjaher, P. Dersin, B. Lamoureux, and N. Zerhouni, "Prognostics and Health Management for Maintenance Practitioners-Review, Implementation and Tools Evaluation," *International Journal of Prognostics and Health Management* 8, no. 3 (2017): 1–31.

7. Y. Langeron, A. Grall, and A. Barros, "A Modeling Framework for Deteriorating Control System and Predictive Maintenance of Actuators," *Reliability Engineering & System Safety* 140 (2015): 22–36.

8. D. R. Obando, J. J. Martinez, and C. Bérenguer, "Deterioration Estimation for Predicting and Controlling RUL of a Friction Drive System," *ISA Transactions* 113 (2021): 97–110.

9. J. Thuillier, M. S. Jha, S. Le Martelot, and D. Theilliol, "Prognostics Aware Control Design for Extended Remaining Useful Life: Application to Liquid Propellant Reusable Rocket Engine," *International Journal of Prognostics and Health Management* 15, no. 1 (2024): 1–14.

10. E. Kipchirchir, M. H. Do, J. G. Njiri, and D. Söffker, "Prognostics-Based Adaptive Control Strategy for Lifetime Control of Wind Turbines," *Wind Energy Science Discussions* 8, no. 4 (2021): 1–16.

11. M. Zagorowska, O. Wu, J. R. Ottewill, M. Reble, and N. F. Thornhill, "A Survey of Models of Degradation for Control Applications," *Annual Reviews in Control* 50 (2020): 150–173.

12. S. Simani and S. Farsoni, *Fault Diagnosis and Sustainable Control of Wind Turbines: Robust Data-Driven and Model-Based Strategies* (Butterworth-Heinemann, 2018).

13. J. Jonkman, "NREL 5-MW Reference Turbine CP, CQ, CT Coefficients, Sheet CpVersusTSR&PitchFAST," (2012), https://forums.nrel.gov/t/nrel-5-mw-reference-turbine-cp-cq-ct-coefficients/456/2.

14. K. E. Johnson, L. Y. Pao, M. J. Balas, and L. J. Fingersh, "Control of Variable-Speed Wind Turbines: Standard and Adaptive Techniques for Maximizing Energy Capture," *IEEE Control Systems Magazine* 26, no. 3 (2006): 70–81.

15. F. D. Bianchi, H. De Battista, and R. J. Mantz, *Wind Turbine Control Systems: Principles, Modelling and Gain Scheduling Design*, vol. 19 (Springer, 2007).

16. M. S. Félix, J. J. Martinez, C. Bérenguer, and K. Tidriri, "Degradation Analysis in a Controlled Flexible Drive Train Subject to Torsional Phenomena Under Different Wind Speed Conditions," in *2022 10th International Conference on Systems and Control (ICSC)* (IEEE, 2022), 90–95.

17. E. E. Romero, J. J. Martinez, and C. Bérenguer, "Degradation of a Wind-Turbine Drive-Train Under Turbulent Conditions: Effect of the Control Law," in *2021 5th International Conference on Control and Fault-Tolerant Systems (SysTol)* (IEEE, 2021), 335–340.

18. M. H. Do and D. Söffker, "Wind Turbine Lifetime Control Using Structural Health Monitoring and Prognosis," *IFAC-PapersOnLine* 53, no. 2 (2020): 12669–12674.

19. M. M. Morato and M. S. Felix, "Data Science and Model Predictive Control: A Survey of Recent Advances on Data-Driven MPC Algorithms," *Journal of Process Control* 144 (2024): 103327, https://doi.org/10.1016/j.jprocont.2024.103327.

20. H. Mo, G. Sansavini, and M. Xie, "Performance-Based Maintenance of Gas Turbines for Reliable Control of Degraded Power Systems," *Mechanical Systems and Signal Processing* 103 (2018): 398–412.

21. J. Pedrosa Alias, V. Puig Cayuela, and F. Nejjari Akhi-Elarab, "Health-Aware Economic MPC for Operational Management of Flow-Based Networks Using Bayesian Networks," *Water (Basel)* 14, no. 10 (2022): 1538.

22. J. Archard, "Contact and Rubbing of Flat Surfaces," *Journal of Applied Physics* 24, no. 8 (1953): 981–988.

23. O. Sename and S. Fergani, "Linear Parameter Varying Systems: From Modelling to Control," in *IVSS 2017-Intelligent Vehicles International Summer School* (IVSS, 2017).

24. D. C. Ramos and P. L. Peres, "A Less Conservative LMI Condition for the Robust Stability of Discrete-Time Uncertain Systems," *Systems & Control Letters* 43, no. 5 (2001): 371–378.

25. D. Liberzon, *Switching in Systems and Control*, vol. 190 (Springer, 2003).

26. S. Boyd, L. El Ghaoui, E. Feron, and V. Balakrishnan, *Linear Matrix Inequalities in System and Control Theory* (SIAM, 1994).

27. F. D. Bianchi, H. De Battista, and R. Mantz, *Wind Turbine Control Systems: Principles, Modelling and Gain Scheduling Design* Advances in Industrial Control Series London (Springer-Verlag London Ltd, 2007).

28. A. Feinberg, *Thermodynamic Degradation Science: Physics of Failure, Accelerated Testing, Fatigue, and Reliability Applications* (John Wiley & Sons, 2016).

29. J. Ma, M. Fouladirad, and A. Grall, "Flexible Wind Speed Generation Model: Markov Chain With an Embedded Diffusion Process," *Energy* 164 (2018): 316–328.

30. S. Pelletier, O. Jabali, G. Laporte, and M. Veneroni, "Battery Degradation and Behaviour for Electric Vehicles: Review and Numerical Analyses of Several Models," *Transportation Research Part B: Methodological* 103 (2017): 158–187.

Appendix A

Table of Variables

Variable	Symbol	Variable	Symbol
Wind speed	v	Wind power	P_{wind}
Average wind	$\overline{v}$	Inertia rotor power	P_r
Wind fluctuation	$\tilde{v}$	Damping of the drivetrain	B_{dt}
Minimum wind turbulence intensity	$\tilde{v}_{min}$	Stiffness of the drivetrain	K_{dt}
Maximum wind turbulence intensity	$\tilde{v}_{max}$	Inertia of the rotor	J_r
Air density	ρ_r	Inertia of the drivetrain	J_g
Rotor radius	R_r	Rotor area	A_r
Power coefficient	C_p	Blade's angle	ϕ
Max. power coefficient	C_p^{max}	Optimal pitch angle	ϕ^{opt}
Operating point power coefficient	$C_p^{\star}$	Tip-speed ratio	λ
GTC controller gain	K_{mppt}	Optimal tip-speed ratio	λ^{opt}
Rotor rotational speed	ω_r	Operating point TSR	$\lambda_{\star}$
Generator rotational speed	ω_g	Degradation level	D
Torsional displacement	θ_{ts}	Estimated degradation level	$\hat{D}$
Rotor torque	τ_r	Maximum degradation level	D_{max}
Generator torque	τ_g	Measured degradation level	Θ_D
Relative differential speed	$\tilde{\omega}$	Median degradation function	$\overline{D}$
Generated energy	E_G	Degradation-rate parameter	β
Generated power	P_G	Estimated degradation-rate parameter	$\hat{\beta}$
Dissipated energy	E_D	Median degradation-rate parameter	$\overline{\beta}$
Dissipated power	P_D	Degradation-rate parameter reference	β^{ref}
Decision time	t_d	Nominal degradation-rate parameter	β^{nom}
End-of-life hitting time	t_f	Manipulable variable	$\mathbf{w}$
End-of-life reference	t_f^{ref}	Nominal manipulable variable value	$\mathbf{w}^{nom}$
Multiplicative uncertainty parameter	γ	Manipulable variable decision vector	$\mathbf{w}^{d}$
Extended multiplicative uncertainty parameter	$\tilde{\gamma}$	Sampling time	T_s
Additional uncertainty parameter	η	RUL median value	$\overline{RUL}$
Inertia model parameter	c	RUL target value	RUL^{ref}
Fluctuation parameter	ϵ	Varying parameter	ρ
Degradation-rate controller gain	K	Polytopic vertices	θ
Degradation state observer gain	L	Convex combination parameter	α
State matrix	A	State cost matrix	Q
Input matrix	B	Control cost matrix	R
Output matrix	C	Stability condition matrix	P
Exogenous system matrix	E	Upper bound cost matrix	W
Input vector	u	Extended state cost matrix	$\mathbf{N}$
State vector	x	Extended control cost matrix	$\mathbf{M}$
Output vector	y	Variable transformation vector	$\mathbf{Y}$
Disturbance vector	w	Optimal controller gain	$\mathbf{K}$
Control integral error	z	Optimal observer gain	$\mathbf{L}$
State estimation error vector	ε	LQR cost function	J
LQR cost vector	h	Average LQR cost function	J_{avg}